Geochemistry, Geophysics, Geosystems®

RESEARCH ARTICLE
10.1029/2021GC010196

Constraints on Early Paleozoic Deep-Ocean Oxygen Concentrations From the Iron Geochemistry of the Bay of Islands Ophiolite

Daniel A. Stolper[1], Xiaofei Pu[2], Max K. Lloyd[1,3], Nikolas I. Christensen[4], Claire E. Bucholz[5], and Rebecca A. Lange[2]

[1]Department of Earth and Planetary Science, University of California, Berkeley, CA, USA, [2]Department of Earth and Environmental Sciences, University of Michigan, Ann Arbor, MI, USA, [3]Department of Geosciences, The Pennsylvania State University, University Park, PA, USA, [4]Department of Earth, Ocean and Atmospheric Sciences, University of British Columbia, Vancouver, BC, Canada, [5]Divison of Geological and Planetary Sciences, California Institute of Technology, Pasadena, CA, USA

Key Points:

- We report $Fe^{3+}/\Sigma Fe$ in volcanic and intrusive crustal rocks and ultramafic rocks from the Early Paleozoic Bay of Islands (BOI) ophiolite
- $Fe^{3+}/\Sigma Fe$ of the BOI volcanic rocks are elevated compared to Precambrian systems but lower than Late Paleozoic to modern systems
- This difference indicates deep-ocean O_2 levels in the Early Paleozoic were elevated compared to the Precambrian but lower than today

Supporting Information:

Supporting Information may be found in the online version of this article.

Correspondence to:

D. A. Stolper,
dstolper@berkeley.edu

Citation:

Stolper, D. A., Pu, X., Lloyd, M. K., Christensen, N. I., Bucholz, C. E., & Lange, R. A. (2022). Constraints on Early Paleozoic deep-ocean oxygen concentrations from the iron geochemistry of the Bay of Islands ophiolite. *Geochemistry, Geophysics, Geosystems*, *23*, e2021GC010196. https://doi.org/10.1029/2021GC010196

Received 4 OCT 2021
Accepted 17 MAY 2022

© 2022 The Authors.
This is an open access article under the terms of the Creative Commons Attribution-NonCommercial License, which permits use, distribution and reproduction in any medium, provided the original work is properly cited and is not used for commercial purposes.

Abstract The deep ocean is generally considered to have changed from anoxic in the Precambrian to oxygenated by the Late Paleozoic (~420–400 Ma) due to changes in atmospheric oxygen concentrations. When the transition occurred, that is, in the Early Paleozoic or not until the Late Paleozoic, is less well constrained. To address this, we measured $Fe^{3+}/\Sigma Fe$ of volcanic rocks, sheeted dykes, gabbros, and ultramafic rocks from the Early Paleozoic (~485 Ma) Bay of Islands (BOI) ophiolite as a proxy for hydrothermal alteration in the presence or absence of O_2 derived from deep marine fluids. Combining this data with previously published data from the BOI indicates that volcanic rocks are oxidized relative to intrusive crustal rocks (0.35 ± 0.02 vs. 0.19 ± 0.01, 1 standard error), which we interpret to indicate that the volcanic section was altered by marine-derived fluids that contained some dissolved O_2. We compare our results directly to the Macquarie Island and Troodos ophiolites, drilled oceanic crust, previously compiled data for ophiolitic volcanic rocks, and newly compiled data for ophiolitic intrusive rocks. These comparisons show that the BOI volcanic (but not intrusive) rocks are oxidized relative to Precambrian equivalents, but are less oxidized relative to Late Paleozoic to modern equivalents. We interpret these results to indicate that the Early Paleozoic ocean contained dissolved O_2, but at concentrations ~2.4× lower than for the Late Paleozoic to today.

1. Introduction

The circulation of seawater through newly formed igneous oceanic crust represents one of the primary means by which the fluid and solid Earth interact and exchange both heat and chemical components (as reviewed in Coogan & Gillis, 2018 and Elderfield & Schultz, 1996). This circulation is generally divided into low- and high-temperature systems. High-temperature hydrothermal systems occur near spreading centers in young oceanic crust (<1 million years) where fluids penetrate and react with rocks at depths of multiple kilometers into the crust (Elderfield & Schultz, 1996). In contrast, low-temperature hydrothermal systems (<100°C) occur throughout shallower volcanic sections for tens of millions of years post crystallization (Coogan & Gillis, 2018; Coogan et al., 2016; Elderfield & Schultz, 1996; Hart & Staudigel, 1978).

Low-temperature circulation of seawater through volcanic sections of oceanic crust results in changes in the chemical composition of these rocks (e.g., Alt et al., 1996; Coggon et al., 2016; Kelley et al., 2003; Staudigel et al., 1996). Specifically, as cold seawater circulates through a volcanic section, igneous minerals are replaced by secondary minerals (as reviewed in Coogan & Gillis, 2018). In the modern ocean, this alteration includes redox reactions in which O_2 dissolved in seawater reacts with and oxidizes reduced sulfur (S^{2-}) to S^{6+} in sulfate and reduced iron as Fe^{2+} to Fe^{3+} (Bach & Edwards, 2003). At the low temperatures at which this alteration occurs (<100°C), sulfate is soluble and is removed from the section lowering the total sulfur content (Bach & Edwards, 2003). In contrast, Fe^{3+} is insoluble and precipitates as secondary iron oxide minerals (primarily Fe-oxyhydroxides). Because the modern deep ocean is oxygenated, low-temperature hydrothermal alteration of volcanic rocks in oceanic crust causes sulfur contents to decrease and the ratio of $Fe^{3+}/(Fe^{2+} + Fe^{3+})$ (here given as $Fe^{3+}/\Sigma Fe$) to increase (Bach & Edwards, 2003; Johnson & Semyan, 1994) relative to their value at crystallization (i.e., the original igneous value). In contrast, deeper sections in oceanic crust (e.g., the sheeted dykes and gabbros) are not as extensively altered by oxygenated low-temperature fluids (Bach & Edwards, 2003). Instead

they are dominantly altered by higher-temperature anoxic fluids that lost their dissolved O_2 earlier in the hydrothermal system via reactions with other igneous rocks. As a consequence, the $Fe^{3+}/\Sigma Fe$ of altered modern sheeted dykes and gabbros are generally lower and closer to the values expected for pristine oceanic crust as compared to hydrothermally altered modern mid-ocean ridge basalts (MORB; Bach & Edwards, 2003). A general review of the processes controlling how iron-bearing igneous minerals become oxidized in oceanic crust during modern hydrothermal circulation is given in Bach and Edwards (2003).

Although the atmosphere and oceans are oxygenated today, this has not always been the case. The Archean atmosphere and oceans are typically thought to have been anoxic (e.g., Canfield, 2005; Farquhar et al., 2000; Lyons et al., 2014; Pavlov & Kasting, 2002). The Paleoproterozoic and Mesoproterozoic are generally modeled to have had atmospheric O_2 contents of order 1% versus modern such that the deep ocean remained anoxic (e.g., Lyons et al., 2014; Planavsky et al., 2018). Sometime in the Neoproterozoic to Early Phanerozoic, it is generally thought that atmospheric O_2 concentrations rose to levels sufficient to oxygenate the deep ocean. Recent studies based on, for example, sedimentary Mo concentrations and Mo isotopic ratios (Dahl et al., 2010), sedimentary Fe speciation (Sperling et al., 2015, 2021), and sedimentary Ce anomalies (Wallace et al., 2017) have been used to argue that the transition to an oxygenated deep ocean occurred in the Paleozoic and potentially not until the late Paleozoic (~420–400 Ma). However, other studies have argued that O_2 concentrations began increasing in the Neoproterozoic (e.g., Blamey et al., 2016; Och & Shields-Zhou, 2012; Sahoo et al., 2012). Such increases in the Neoproterozoic are sometimes interpreted as transient events as opposed to a stepwise oxygenation event such that marine O_2 concentrations varied spatially and temporally in the Neoproterozoic and Early Paleozoic (e.g., Kendall et al., 2015; Reinhard & Planavsky, 2022; Sahoo et al., 2016; Tostevin & Mills, 2020). If, as is usually assumed, deep-ocean oxygen concentrations are largely controlled by atmospheric O_2 concentrations (Canfield, 1998; Lyons et al., 2014), this timeline would require a delay of hundreds of millions of years between the processes that caused atmospheric oxygen levels to begin increasing (once or multiple times if dynamic) over background Paleoproterozoic and Mesoproterozoic levels and the final increase in atmospheric O_2 concentrations to levels sufficient to oxygenate the deep ocean. Why such a delay may have occurred is not known, but various ideas on what caused the final increase in atmospheric O_2 levels to values that resulted in the oxygenation of the deep ocean include the rise of land plants (Lenton et al., 2016; Wallace et al., 2017), changes in internal feedbacks in global biogeochemical cycles (Alcott et al., 2019), or changes in the size of igneous O_2 sinks (Stolper et al., 2021). These ideas are generally predicated on a positive dependence of deep ocean O_2 concentrations on atmopsheric O_2 levels. Finally, we note that there remains debate on the fidelity of some of the geochemical records used to reconstruct past marine and atmospheric O_2 (Planavsky et al., 2020; Slotznick et al., 2018, 2019; Yeung, 2017).

Given this history of deep-ocean O_2 concentrations, Stolper and Keller (2018) proposed that the $Fe^{3+}/\Sigma Fe$ of altered submarine volcanic rocks should be lower when the deep ocean was anoxic versus in an oxygenated deep ocean as there would be no dissolved O_2 to oxidize the igneous rocks during hydrothermal alteration. On this basis, they proposed that the $Fe^{3+}/\Sigma Fe$ of ancient altered submarine volcanic rocks could be a proxy for deep-ocean O_2 concentrations. To explore this, they compiled $Fe^{3+}/\Sigma Fe$ ratios of submarine volcanic rocks preserved in previously identified ophiolite sequences from the Archean to today. They found that for Precambrian-aged rocks, when the deep ocean is thought to have been anoxic, $Fe^{3+}/\Sigma Fe$ of submarine volcanic rocks are low, and similar to the average value of modern day unaltered MORB. In contrast, for Phanerozoic-aged rocks, when the deep ocean is thought to have been oxygenated, $Fe^{3+}/\Sigma Fe$ of submarine volcanic rocks are elevated. Stolper and Keller (2018) proposed that this change was due to the increase in deep-ocean O_2 concentrations between the Proterozoic and Phanerozoic (and thus consistent with the studies discussed above) that then allowed O_2 to begin flowing into the volcanic section of oceanic crust during hydrothermal alteration. This, in turn, caused the oxidation of iron in the relatively reduced igneous rocks on the ocean floor.

In that study, Stolper and Keller (2018) also examined differences in volcanic rocks from the Early Paleozoic (541–420 Ma) versus older and younger rocks. They found that volcanic rocks from the Late Paleozoic (and also the Mesozoic-Cenozoic) showed clear elevation in $Fe^{3+}/\Sigma Fe$ versus Precambrian equivalents. However, the volcanic rocks from the Early Paleozoic, though somewhat elevated in $Fe^{3+}/\Sigma Fe$, had mean $Fe^{3+}/\Sigma Fe$ values and distributions that were not demonstrably different from the Precambrian rocks with lower $Fe^{3+}/\Sigma Fe$. On this basis, Stolper and Keller (2018) proposed that it was "probably" not until the Late Paleozoic that O_2 concentrations reached sufficient levels to clearly oxidize volcanic rocks — that is, there may have been a shift in the Early Paleozoic in terms of volcanic $Fe^{3+}/\Sigma Fe$, but it was not until the Late Paleozoic to modern that this shift became

readily apparent. This was consistent with and provided independent evidence for the prior work described above that indicated that the deep ocean did not become oxygenated until the Late Paleozoic (Dahl et al., 2010; Sperling et al., 2015).

Understanding precisely when the deep ocean became oxygenated is important to a variety of problems ranging from the evolution and diversification of animals (see review in Wood et al., 2020) to changes in the composition of subducted components to the mantle and the origin of porphyry copper deposits and oxidized island-arc rocks (Evans, 2012; Richards, 2015; Stolper & Bucholz, 2019). An approach that many of the studies above have used to conclude that the deep ocean did not become oxygenated until the Late Paleozoic are based on data compilations from a variety of settings that allow one to observe changes in mean trends over time (Dahl et al., 2010; Sperling et al., 2015; Stolper & Keller, 2018; Tostevin & Mills, 2020; Wallace et al., 2017). This approach has the advantage of removing potential biases associated with the paleoceanographic conditions and potentially later alteration that may have occurred at a specific study site and thus provide, hopefully, a better estimate of the mean state of the Earth. An alternative approach is to examine one geologic formation in detail and test whether, at the individual formational level, conclusions drawn from a mean trend are consistent with a specific system. This has the disadvantage that any conclusions are fundamentally local. But it allows for a careful examination of systematics of a given proxy when holding the study location constant. Such a detailed study has not been done for $Fe^{3+}/\Sigma Fe$ as a proxy for marine O_2 concentrations in the Paleozoic or in older rocks. To address this, we present $Fe^{3+}/\Sigma Fe$ of hydrothermally altered igneous rocks from the Early Phanerozoic (~485 Ma) Bay of Islands (BOI) ophiolite to examine whether, at this time, oxidative alteration of volcanic rocks was as intense as seen in Late Paleozoic to modern rocks, more similar to the Precambrian, or intermediate. As such, this system serves as a test of whether in the Early Paleozoic deep-ocean O_2 levels were or were not sufficiently high to allow for measurable oxidation of submarine basalts during hydrothermal alteration.

2. The Bay of Islands Ophiolite

2.1. Geologic Background

The BOI ophiolite complex (Newfoundland) is a "Penrose" style ophiolite with some massifs (North Arm Mountain and Blow-Me-Down Mountain) containing complete sections that include peridotites, gabbros, sheeted dykes, and volcanic rocks (Cawood & Suhr, 1992; Church & Stevens, 1971; Dewey & Casey, 2013; Williams, 1973). It is commonly used as a model for the formation and obduction of ophiolites (Cawood & Suhr, 1992), low-temperature alteration of igneous rocks (Jacobsen & Wasserburg, 1979; Parendo et al., 2017), as well as a proxy for the properties of oceanic crust (e.g., Christensen & Salisbury, 1982).

BOI igneous rocks formed in a subduction zone setting at ~485 Ma (Cawood & Suhr, 1992; Dewey & Casey, 2013. Assignment to a subduction zone setting is based on the geochemistry of the igneous rocks (Elthon, 1991; Jenner et al., 1991). The generally quoted formation age of ~485 Ma is based on U/Pb zircon ages from a trondhjemite ($485.7^{+1.9}_{-1.2}$ Ma; 2σ) (Dunning & Krogh, 1985) as well as 484 ± 5 Ma based on U/Pb dating of zircon and baddeleyite from a gabbro (Jenner et al., 1991). Here we follow Dewey and Casey (2013) and use an age of ~485 Ma for the formation of the igneous rocks. Yan and Casey (2020) recently revisited these ages using laser ablation inductively coupled plasma U-Pb dating of zircons from trondhjemites and derived an age of 488.3 ± 1.5 (2σ) which is within uncertainty of prior estimates. We note that there is not a singular age for the various igneous rocks in the ophiolite as they will have formed over millions of years when spreading was active.

The BOI igneous rocks obducted onto Laurentia during the Taconic Orogeny (Cawood & Suhr, 1992). The age of obduction is generally given as ~470 Ma and, as summarized in Cawood and Suhr (1992) and Yan and Casey (2020), is based on hornblende $^{40}Ar/^{39}Ar$ cooling ages (Dallmeyer & Williams, 1975) from the metamorphic sole and amphibolite K-Ar ages (Archibald & Farrar, 1976).

The paleolatitude of the BOI igneous rocks at the time of formation is not, to our knowledge, known. General paleogeographical constraints as follows. At the time of obduction (~470 Ma) onto Newfoundland, Newfoundland's paleolatitude (as part of Laurentia) was between 0 and 10°S with the Iapetus Ocean to the south (Swanson-Hysell & Macdonald, 2017). The various accreted terranes that form the Taconic orogeny (which includes the BOI) are derived from the collision of arcs generated in the Iapetus Ocean (and thus in the southerly direction) (Mac Niocaill et al., 1997; Swanson-Hysell & Macdonald, 2017). On this basis, we can place the likely formational location of the BOI southward of the equator and in the Iapetus Ocean.

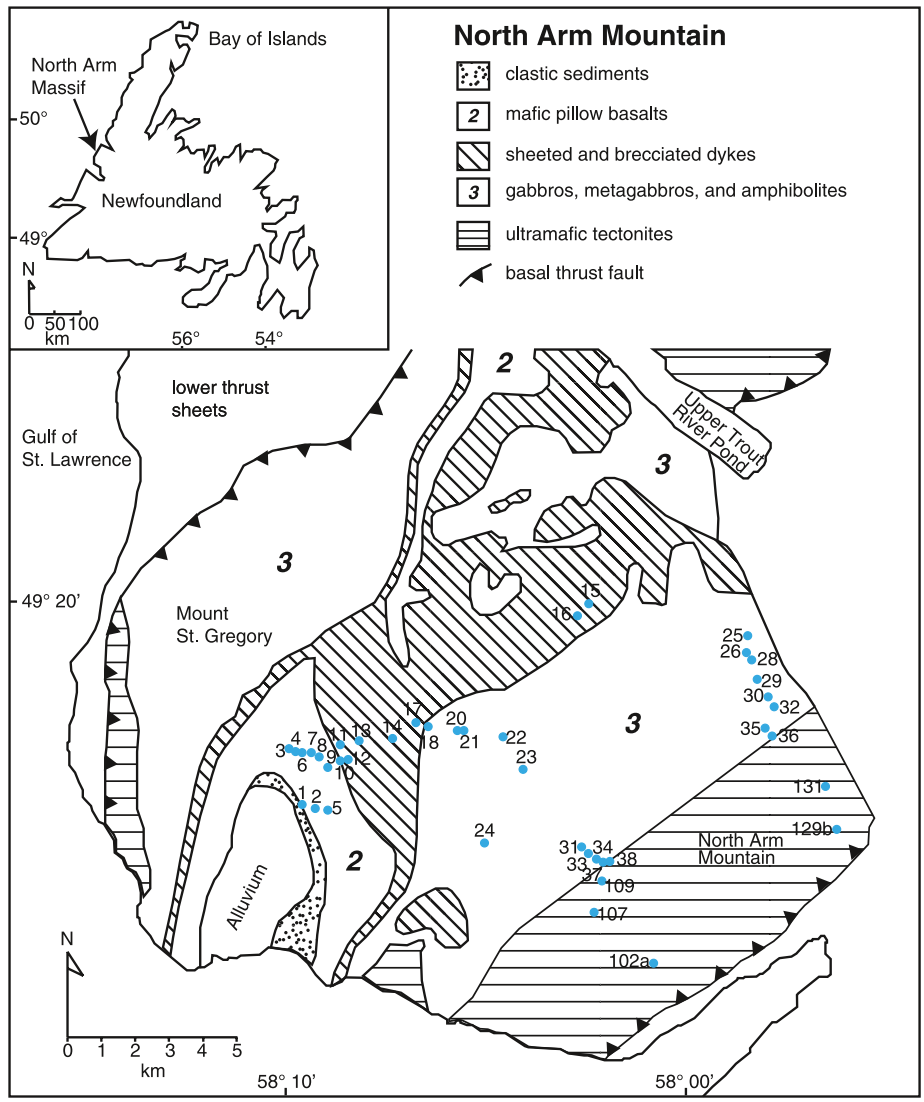

Figure 1. Map of the North Arm Massif of the Bay of Islands ophiolite. Blue circles are the samples measured here as originally described in Christensen and Salisbury (1982) and the map is modified from that study.

The paleoceanographic context of the BOI formational environment is also not well constrained. Casey et al. (1985) suggested the igneous rocks may have formed in an open-ocean setting based on the presence of radiolarian cherts interstratified in pillow basalts. However, we are unaware of any quantitative constraints on water depth or further details of the paleoenvironment.

Finally, the system is known to have experienced hydrothermal alteration by seawater down to the gabbroic section based on mineral assemblages (Williams & Malpas, 1972), presence of volcanogenic massive sulfides (Duke & Hutchinson, 1974), and the strontium (Jacobsen & Wasserburg, 1979) and potassium (Parendo et al., 2017) isotope systematics of the igneous rocks.

2.2. Samples

We measured the same samples (n = 41) described in Christensen and Salisbury (1982) from the North Arm Massif of the BOI. All samples were from cored material (~2 cm in diameter and 6 cm in length) subsampled from larger hand samples taken from outcrops and stored since their original collection. Lithologies include volcanic rocks, sheeted dykes, gabbros, and serpentinized peridotites that, together, span ~9 km of depth into the crust and upper mantle lithosphere (Figure 1). Samples and the basis for emplacement depth assignments are

described in detail in and taken from Christensen and Salisbury (1982). Christensen and Salisbury (1982) give depths relative to the sediment-basalt contact and interpret sediments as conformably overlying the pillow basalts (as also interpreted in the original mapping of Williams, 1973; as well as the work of Malpas, 1977). In contrast, Casey and Kidd (1981) interpreted most of the overlying sediments as forming on top of an erosion surface and thus unrelated to the initial formation of the ophiolite — Casey et al. (1981) note that conformable sediments do overly the volcanic sequence in the North Arm massif in one area. We have preserved the original depth assignments of Christensen and Salisbury (1982).

3. Methods

As samples had been in storage in air for ∼40 years, exteriors were removed to eliminate any potential surface oxidation (which was not observed to be visually present). Specifically, at UC Berkeley, outer surfaces were first shaved with a diamond-coated abrasion saw. The remaining cores were then rinsed in flowing water and dried with compressed air. For $Fe^{3+}/\Sigma Fe$ determinations, samples were manually crushed with 5–8 taps in a tungsten-carbide-lined percussion mortar and mm-sized grains collected. This was done to avoid the oxidation of iron that can occur during automated rock crushing and milling (Fitton & Gill, 1970). For major and trace element analyses, a separate split of the sample was powdered in an agate griding vessel in a planetary ball mill at Caltech.

Fe^{2+} concentrations (as FeO) in the 41 samples were analyzed at the University of Michigan over five analytical sessions following the titration method of Wilson (1960). A subset of samples ($n = 19$) were analyzed in duplicate or triplicate and yielded a pooled standard deviation for FeO analyses of 0.15 wt. % (1σ). Accuracy and reproducibility were verified by analyzing two US Geological Survey standards, BIR-1 and W-2a, in duplicate in each analytical session (12 and 8 replicates, respectively). The resulting averages were 8.40 (±0.17; 1σ) and 8.38 (±0.18) wt. % FeO respectively and match the certified concentration of 8.30 wt. % FeO for both standards. We note that one sample (129-Ba) exhibited a worse reproducibility than typical (standard deviation of 0.7 wt. % FeO on two replicates). This sample is a serpentinite and this elevated uncertainty does not impact any interpretations presented below.

We measured the major and trace element geochemistry of splits from the same samples measured for FeO contents at Caltech using a 4 kW Zetium Panalytical X-ray fluorescence spectrometer following the methods of Bucholz and Spencer (2019). One sample was not measured for major and trace element geochemistry at Caltech (31–116, a wehrlite from 5.9 km depth) due to insufficient sample. We additionally report major and trace element geochemistry where available on some samples made by the X-Ray Assay Laboratories at the University of Washington (though from different sample splits vs. those studied here) — these measurements were made in the 1980s as part of the initial characterization of these rocks, but were never published.

4. Results

4.1. Bay of Islands Samples Measured in This Study

The geochemistry of the individual samples is given in Data Set S1 in Supporting Information S1. We generally have calculated $Fe^{3+}/\Sigma Fe$ using the total Fe measured at Caltech. For sample 31–116, we use the University of Washington total Fe determination as this sample was not measured at Caltech for major element geochemistry (see Methods). Additionally, for three gabbroic rocks, using the Caltech major element determinations yields Fe^{2+} concentrations that are larger than the total Fe concentration. These samples contain the lowest measured total iron contents (≤3% as determined at Caltech). For two of these samples, XRF measurements made at the University of Washington yielded total Fe greater than Fe^{2+} and were used to calculate $Fe^{3+}/\Sigma Fe$ for these instances. However, for one sample (34–114), Fe^{2+} contents are still larger than total Fe measurements regardless of where the total Fe was measured and this sample is not discussed further.

We do not believe that these specific results, that is, Fe^{2+} greater than total Fe, are due to analytical issues. For example, FeO determinations on USGS standards are within 0.1 wt. % of accepted values and sample FeO determinations are generally reproducible (1σ of 0.15 wt. %). Additionally total iron contents measured on different aliquots of samples in different labs ∼40 years apart are in general agreement. Specifically, total Fe measured on different aliquots of hand samples at the University of Washington and Caltech differ, on average, by 0.05 wt. % Fe (with the University of Washington higher) and yield a slope of 0.88 (x = Caltech, y = University of

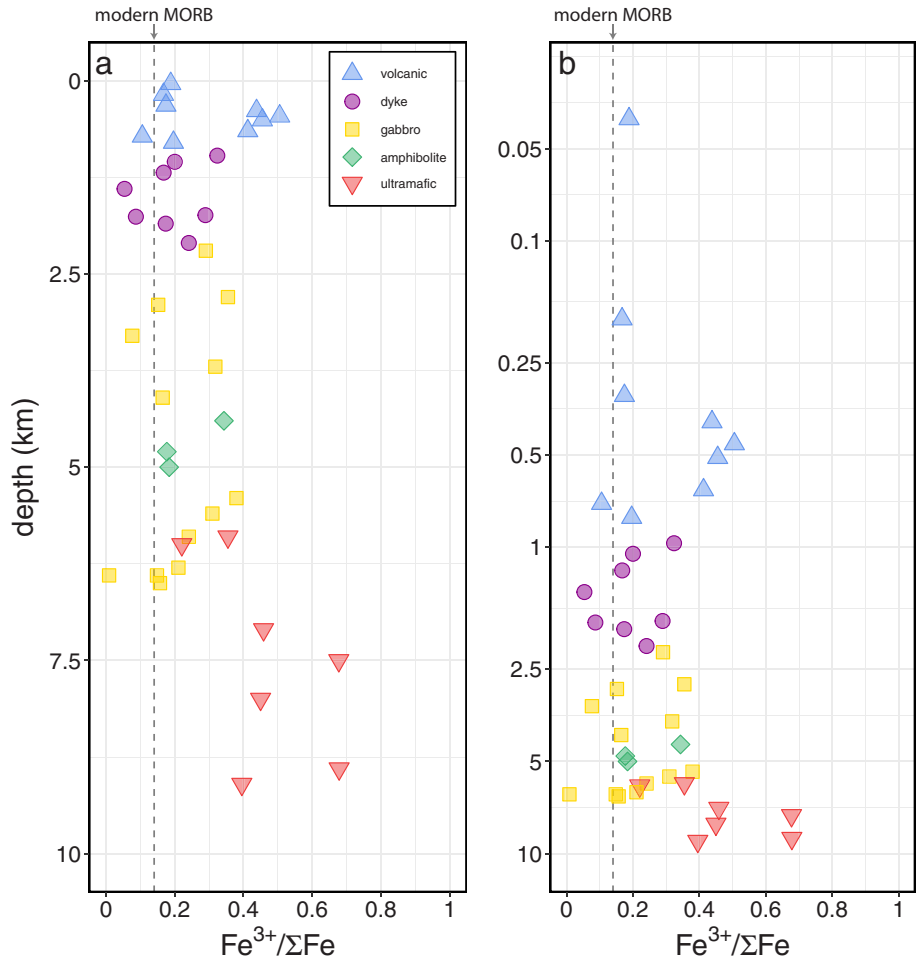

Figure 2. $Fe^{3+}/\Sigma Fe$ of various rock types from the Bay of Islands versus depth below the sediment-basalt interface on a linear (a) and logarithmic (b) depth scale. The vertical dotted line is the average $Fe^{3+}/\Sigma Fe$ of mid-ocean ridge basalt glasses from Zhang et al. (2018).

Washington) with an uncertainty of ±0.06 (1 standard error [s.e.]) and thus within ±2 s.e. of a slope of 1 (Figure S1 in Supporting Information S1). However, there is variability in total Fe determinations between labs with a standard deviation of the difference between the two of 0.76 wt. % Fe. Our interpretation of this is that these differences are real and reflect heterogeneity in total iron contents that exist at the scale of some hand samples. Based on this, we propose that we may have generated variability between the geochemistry of samples lightly crushed for Fe^{2+} analyses versus the samples ground for XRF analyses — different aliquots were taken for these different analyses (see Methods). Such variability could create the potential for measured Fe^{2+} contents greater than the total Fe when samples have both low $Fe^{3+}/\Sigma Fe$ and have low total Fe as was the case for the three gabbroic samples discussed above.

In Figure 2 we plot the variation in $Fe^{3+}/\Sigma Fe$ as a function of depth below the sediment-basalt interface. Before examining the structure of the data versus depth, we first compare mean values of the various lithologies. Mean $Fe^{3+}/\Sigma Fe$ of the volcanic rocks is 0.29 ± 0.05 (1 s.e., $n = 9$) versus 0.21 ± 0.02 ($n = 24$) for the intrusive rocks (i.e., dykes, amphibolites, and gabbros). The amphibolites examined here are found in the gabbroic section. They have been interpreted to have formed when seawater flowed along fractures and shear zones at this depth (Christensen & Salisbury, 1982). For the intrusive rocks more specifically: the dyke $Fe^{3+}/\Sigma Fe$ mean is 0.19 ± 0.03 (1 s.e., $n = 8$), the gabbro mean is 0.22 ± 0.03 ($n = 13$), and the amphibolite mean is 0.23 ± 0.05 ($n = 3$). Finally, the ultramafic rocks yield a mean value of 0.46 ± 0.06 (1 s.e., $n = 7$). For comparison, typical mid-ocean ridge, back-arc basin, and forearc glasses show a range of ~0.14–0.20 (Brounce et al., 2014, 2015; Cottrell & Kelley, 2011).

The high (>0.4) $Fe^{3+}/\Sigma Fe$ of altered ultramafic rocks is common in ophiolites (e.g., Evans, 2012) and is thought to be caused by fluid-mediated oxidative serpentinization reactions during initial hydrothermal circulation near the spreading center, during hydrothermal processes associated with obduction, and/or by meteoric alteration. This oxidation is disconnected from marine O_2 levels and occurs in anoxic fluids (e.g., Bach & Edwards, 2003; Neal & Stanger, 1983; Stevens & McKinley, 2000). As such, the high $Fe^{3+}/\Sigma Fe$ of the ultramafic rocks is not discussed further as, based on this, their $Fe^{3+}/\Sigma Fe$ does not provide a constraint on the presence of absence of O_2 in the altering fluids.

In identifying whether ophiolite volcanic rocks were oxidized by dissolved O_2 during hydrothermal alteration on the seafloor, we consider it useful to compare such rocks to intrusive rocks from the same system as opposed to modern basalts or glasses. This is because ophiolite rocks may have experienced oxidation following hydrothermal alteration due to, for example, oxidation on Earth's surface by atmospheric O_2 or some amount of oxidation via serpentinization of the igneous minerals. We propose that looking at relative differences in $Fe^{3+}/\Sigma Fe$ between volcanic and intrusive rocks from the same setting (and exposed at the surface today) can act to normalize for any of this later oxidative alteration. Implicit in doing this comparison is the assumption that the intrusive sections are not strongly oxidized by O_2 during hydrothermal alteration. This appears to commonly be the case (Bach & Edwards, 2003).

At BOI, we observe a slight elevation in the average $Fe^{3+}/\Sigma Fe$ of the volcanic versus intrusive rocks with a difference of 0.09 ± 0.06 (± 1 s.e.; with volcanic rocks elevated). This difference is not distinguishable from zero at the ± 2 s.e. level and thus it is not clear if, on average, the studied BOI volcanic rocks are meaningfully oxidized as compared to the intrusive rocks. However, the depth distribution of $Fe^{3+}/\Sigma Fe$ indicates that this difference may be meaningful. Specifically, five of the volcanic rocks have $Fe^{3+}/\Sigma Fe$ of 0.1–0.2 and are found in the top 320 m and bottom 720–800 m of the volcanic section. These values scatter around that for modern MORB (Cottrell & Kelley, 2011; Zhang et al., 2018) and, as such, we consider these samples to be relatively unaltered in terms of $Fe^{3+}/\Sigma Fe$ from the original values at crystallization. In contrast, from 390 to 650 m depth, $Fe^{3+}/\Sigma Fe$ of the volcanic rocks range from 0.41 to 0.51 which, other than the ultramafic rocks, are the highest values in the BOI ophiolite measured here (the next highest sample is a gabbro at 0.38). As such, these samples are indicative of oxidative alteration post crystallization focused at this depth range (discussed in detail below).

We also provide in Figure 3 K_2O contents versus depth. We use K_2O as a proxy for low-temperature alteration that is independent of the O_2 content of the deep ocean. During low-temperature hydrothermal alteration of oceanic crust, seawater-derived potassium can be taken up in secondary minerals, increasing total K_2O concentrations over initial igneous values set at crystallization (Hart & Staudigel, 1982). For this study, it is important to know if samples have been hydrothermally altered as, if a sample displays low $Fe^{3+}/\Sigma Fe$, it could be caused either because samples were not altered by hydrothermal flow or were altered but the fluid was anoxic. As seen in Figure 3, samples from the shallowest part of the section (top 320 m), all have elevated K_2O (0.55–0.91 wt.%) versus mean values of various forms of MORB with average N-MORB = 0.14%, D-MORB = 0.096%, and E-MORB = 0.394% and back-arc basin basalts = 0.236% (Gale et al., 2013) indicating hydrothermal alteration by seawater occurred that did not cause oxidation of iron in these samples.

4.2. Bay of Islands Samples Measured in This Study Versus Presented in Prior Work

As part of this work, we also compiled an additional 99 BOI $Fe^{3+}/\Sigma Fe$ measurements (24 volcanic and 75 intrusive rocks; data given in Data Set S2 in Supporting Information S1) (data from Coish, 1977; Duke & Hutchinson, 1974; Malpas, 1976; Williams & Malpas, 1972). Emplacement depths for these samples are not available, but the rock types are. As such, we can compare $Fe^{3+}/\Sigma Fe$ of volcanic versus intrusive rocks (Figure 4). Mean $Fe^{3+}/\Sigma Fe$ of intrusive rocks for the two datasets do not differ beyond ± 2 s.e.: 0.21 ± 0.02 (1 s.e., $n = 24$) as measured here versus 0.19 ± 0.01 ($n = 75$) for the compilation. Histograms of the intrusive data (Figures 4c and 4d) are also similar with peak $Fe^{3+}/\Sigma Fe$ distributions between 0.1 and 0.3. Means for the volcanic rocks also do not differ at the ± 2 s.e. level: 0.29 ± 0.05 (± 1 s.e., $n = 9$) as measured here versus 0.37 ± 0.03 ($n = 24$) in the compilation. Although the means do not differ beyond ± 2 s.e., the compiled data demonstrates an important point — the relatively oxidized samples measured here ($Fe^{3+}/\Sigma Fe > 0.3$) are not anomalous compared to other volcanic samples from the BOI. Rather, in the newly compiled data most (79%) of the volcanic rocks are similarly oxidized ($Fe^{3+}/\Sigma Fe > 0.3$) — this skew to somewhat elevated $Fe^{3+}/\Sigma Fe$ (>0.3) is also seen in the histograms (Figures 4a and 4b).

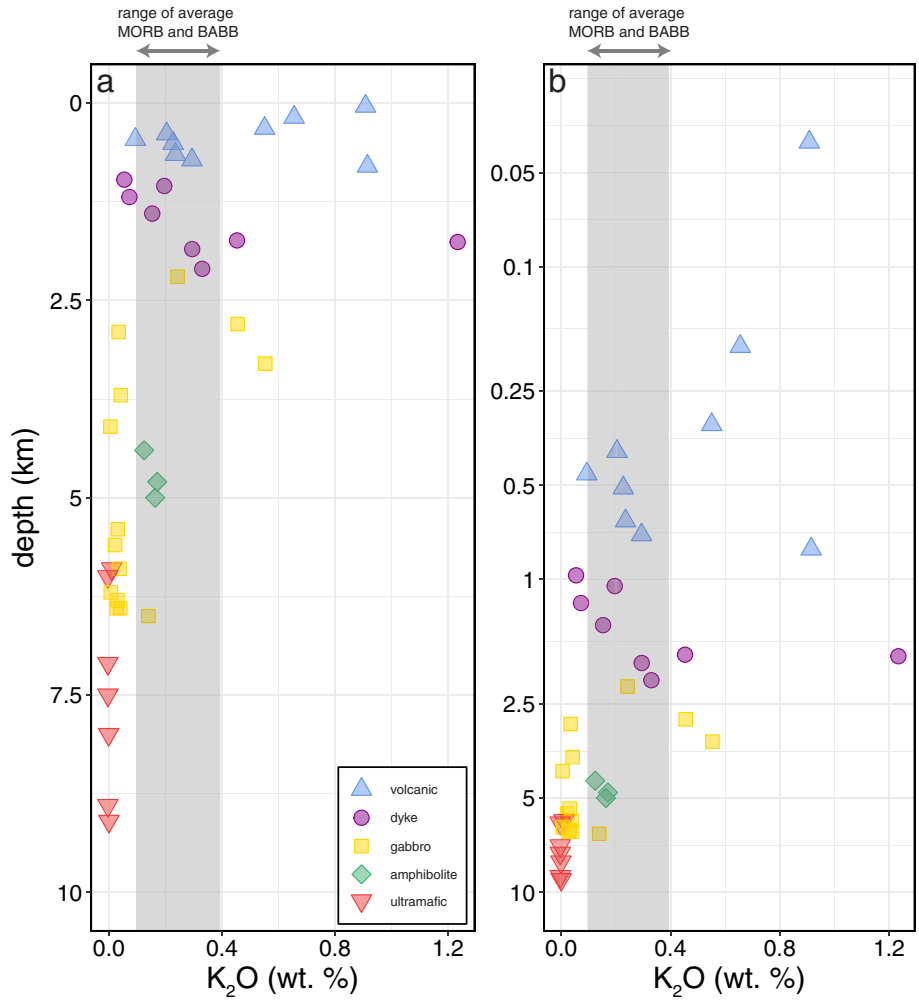

Figure 3. K_2O of various rock types from the Bay of Islands versus depth below the sediment-basalt interface on a linear (a) and logarithmic (b) depth scale. The gray rectangle is the range of primary K_2O contents of mid-ocean ridge basalts and back-arc basin basalts from Gale et al. (2013).

5. Comparison of BOI Data to Other Ophiolites and Oceanic Crust

5.1. Comparison of $Fe^{3+}/\Sigma Fe$ Versus Depth for BOI With Mesozoic and Cenozoic Ophiolites and Drilled Oceanic Crust

Before interpreting the BOI results in terms of their connection to Early Paleozoic ocean chemistry, we first place these results into a wider context. In this subsection, we compare the variations in $Fe^{3+}/\Sigma Fe$ versus depth at BOI to equivalent data from Mesozoic and Cenozoic ophiolites and drilled oceanic crust. We do this as it is generally understood that atmospheric O_2 levels were sufficiently high in the Mesozoic and Cenozoic to keep the deep ocean oxygenated (e.g., Lyons et al., 2014). As such, these systems provide a comparison point for BOI samples to a boundary condition of approximately modern concentrations of O_2 in the deep ocean — we note that we are unaware of data sets for older time frames that allow for such a comparison versus depth, which is why only a comparison to Mesozoic and younger systems is made. Following this and in the next subsection, we compare the BOI data to compiled data from ophiolites without depth assignments but as a function of rock type (intrusive vs. extrusive) with ages going back to ~3.5 billion years.

We compare the BOI $Fe^{3+}/\Sigma Fe$ versus depth data to equivalent data from three younger systems: the Cenozoic Macquarie Island ophiolite, the Cretaceous Troodos ophiolite, and Mesozoic to Cenozoic volcanic rocks from drilled ocean cores as well as the Site 504B drill core that sampled both volcanic rocks and sheeted dykes of 5.9 million year old oceanic crust — these systems are described in more detail below. These ophiolites and oceanic

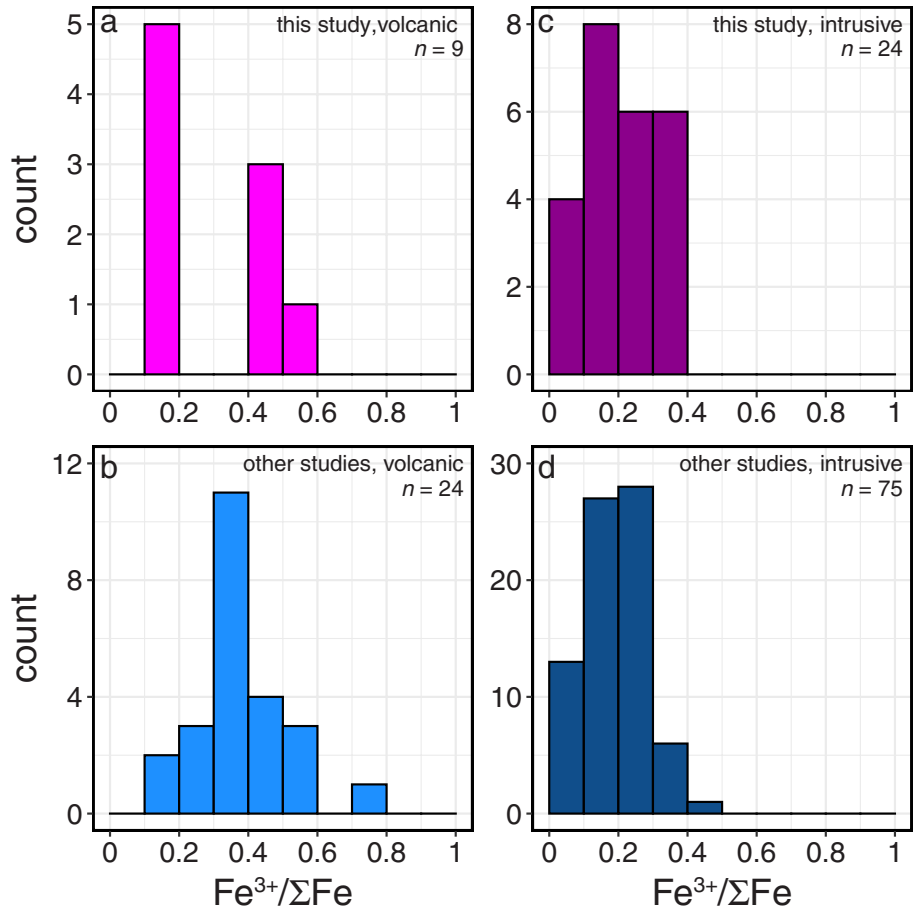

Figure 4. Comparison of $Fe^{3+}/\Sigma Fe$ from volcanic (a) and intrusive (c) rocks from this study versus our compilation of data from other studies (b and d).

crust have $Fe^{3+}/\Sigma Fe$ that can be plotted as a function of depth below the sediment-basalt contact. In doing this comparison, we only include and discuss in this subsection BOI samples measured in this study as work from other studies do not have known depths. These comparisons are made in Figure 5 and depth is provided both on a linear and logarithmic scale. We do not include ultramafic rocks in this comparison. In all cases, we lump rocks from the transition zone where pillows and sheeted dykes co-occur (i.e., between the base of the volcanic section and top of the sheeted dyke complex) with rocks from the sheeted dyke complex for simplicity.

We first compare the BOI to the Macquarie Island ophiolite (Figures 5a and 5b). The Macquarie Island ophiolite is ~10 million years old and is considered to represent obducted oceanic crust formed at a mid-ocean ridge (as opposed to a subduction zone setting as is the case for BOI) (Varne et al., 2000). Based on major and trace element geochemistry as well as $^{87}Sr/^{86}Sr$ and $\delta^{18}O$, the system was hydrothermally altered by seawater through to the gabbroic layer (Coggon, 2006; Coggon et al., 2016). $Fe^{3+}/\Sigma Fe$ data for the Macquarie Island ophiolite are taken from Rutter (2015). $Fe^{3+}/\Sigma Fe$ of intrusive rocks from both ophiolites overlap within ±2 s.e.: 0.21 ± 0.02 (1 s.e., n = 24) for BOI versus 0.19 ± 0.01 (n = 22) for Macquarie Island. In contrast, the mean BOI volcanic rocks are lower in $Fe^{3+}/\Sigma Fe$ as compared to those at Macquarie Island and do not overlap at the ±2 s.e. level: 0.29 ± 0.05 (1 s.e., n = 9) for BOI versus 0.47 ± 0.03 (n = 15) for Macquarie Island. These values yield calculated mean differences in $Fe^{3+}/\Sigma Fe$ for volcanic versus intrusive sections at Macquarie Island of 0.28 ± 0.03 (1 s.e.) as compared to 0.09 ± 0.06 at BOI. As such, although the two intrusive sections are similar in $Fe^{3+}/\Sigma Fe$, the Macquarie Island volcanic rocks are, on average, significantly more oxidized than those from BOI as measured here.

The BOI and Macquarie Island ophiolites also differ in how $Fe^{3+}/\Sigma Fe$ in the volcanic section varies as a function of depth. Specifically, all volcanic rocks at Macquarie Island over the top 800 m have elevated $Fe^{3+}/\Sigma Fe$ (>0.37)

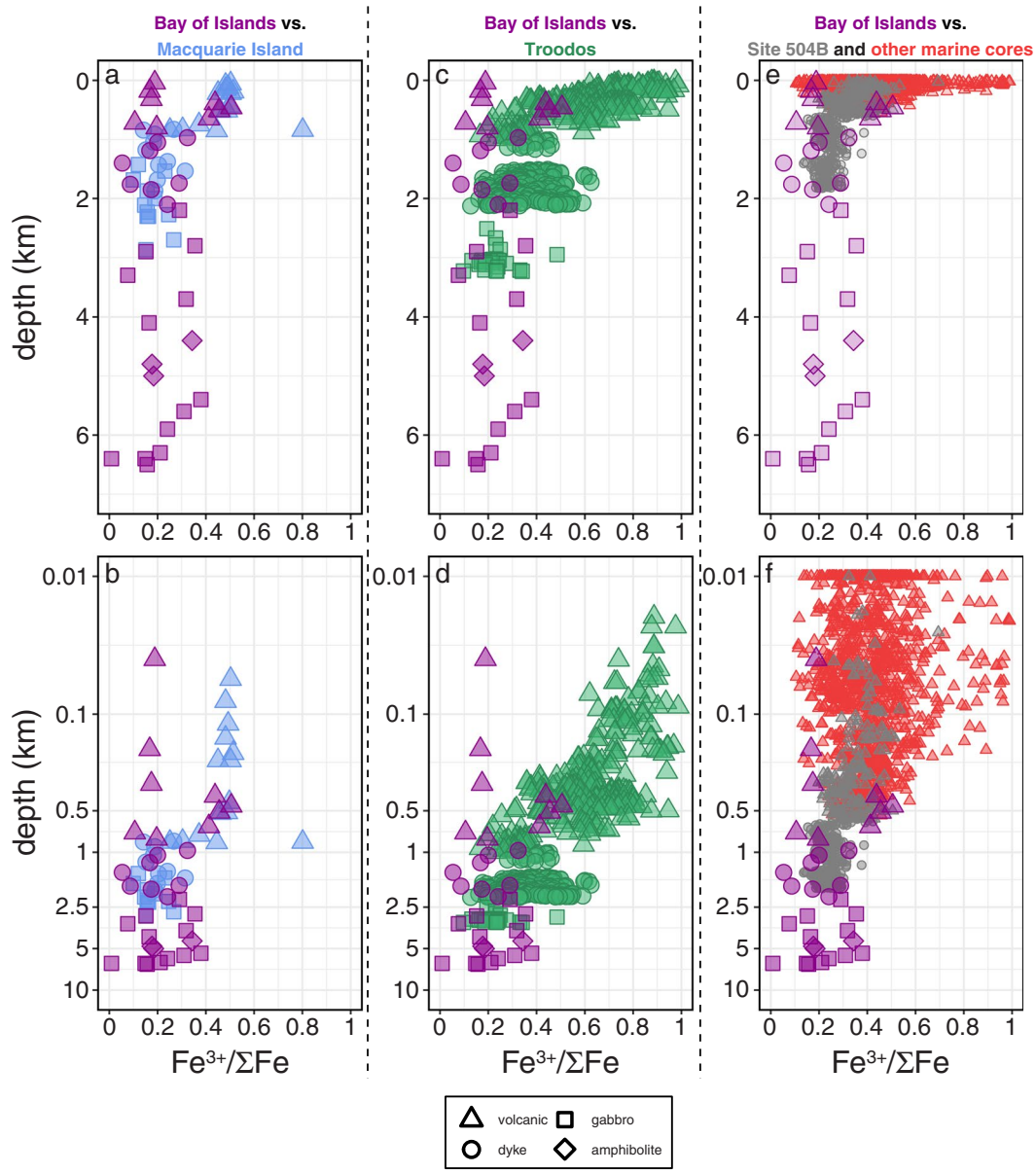

Figure 5. Comparison of Bay of Islands $Fe^{3+}/\Sigma Fe$ as a function of depth below the sediment-basalt interface (linear versus depth for top panels and logarithmic for bottom panels) versus in (a) and (b) the Macquarie Island ophiolite (Rutter, 2015); (c) and (d) the Troodos Ophiolite (Gibson et al., 1989, 1991; Robinson et al., 1987); and (e) and (f) cored volcanic rocks from the seafloor (data from compilation given in Stolper & Keller, 2018) and cored volcanic and intrusive rocks from Site 504B (Alt et al., 1996). Symbols are the same as in Figures 2 and 3 and given in the legend. Colors correspond to the location of the sample and are given by the text color for the location at the top of the figures.

— only the deepest measured Macquarie Island volcanic rock (850 m) has a lower $Fe^{3+}/\Sigma Fe$ (0.25). In contrast, as discussed above, BOI volcanic rocks do not show a uniform elevation in $Fe^{3+}/\Sigma Fe$ versus the intrusive section. Instead the oxidation is concentrated in the middle of the volcanic section.

We next compare our BOI data to the Troodos ophiolite (Figures 5c and 5d). The Troodos ophiolite is Cretaceous in age (~90 Ma) and formed in a suprasubduction zone setting (Osozawa et al., 2012) and is thus comparable in its formational setting to that of the BOI. Measurements are derived from the reports of the Cyprus Crustal Study Project (Gibson et al., 1989, 1991; Robinson et al., 1987). Unlike the Macquarie Island ophiolite, the intrusive mafic rocks from Troodos are elevated in $Fe^{3+}/\Sigma Fe$ compared to those from BOI: 0.34 ± 0.01 (1 s.e., $n = 218$) at Troodos versus 0.21 ± 0.02 ($n = 24$) at BOI. This difference is dominantly due to more oxidation in the sheeted

dyke complex at Troodos, which yields a mean $Fe^{3+}/\Sigma Fe$ of 0.36 ± 0.01 (1 s.e., n = 188) versus 0.23 ± 0.01 (n = 30) for the gabbros. This indicates that at Troodos as compared to both BOI and Macquarie Island, oxidizing fluids penetrated to depths greater than 1 km and that oxidation can occur at depths below the volcanic section. This oxidation could be due to O_2 reaching this section or, alternatively, as the sheeted dyke complex is generally altered at elevated temperatures (>200°C; e.g., Alt et al., 1996), could be due the oxidation of iron by sulfate, which is known to occur (based on experiments) at temperatures above 200°C (Shanks et al., 1981).

Troodos volcanic rocks are significantly more oxidized than Troodos intrusive rocks and are more oxidized than volcanic and intrusive rocks from BOI (as visually apparent in Figures 5c and 5d). Specifically, volcanic rocks from Troodos have an average $Fe^{3+}/\Sigma Fe$ of 0.62 ± 0.01 (1 s.e., n = 277) versus 0.29 ± 0.05 (n = 9) for BOI. Differences in $Fe^{3+}/\Sigma Fe$ at Troodos versus BOI for volcanic versus intrusive rocks are 0.28 ± 0.01 versus 0.09 ± 0.06 respectively. The difference of 0.28 at Troodos is the same as that at Macquarie Island.

The differences at Troodos versus BOI are also apparent in examinations of $Fe^{3+}/\Sigma Fe$ versus depth. At Troodos, $Fe^{3+}/\Sigma Fe$ decreases with increasing depth in the volcanic section. This change is likely caused by hydrothermal fluids being able to more easily penetrate the top of the volcanic section (and thus see fluid flow for longer) than deeper sections due to differences in porosity and permeability as well as access to fresh seawater (Coogan & Gillis, 2018). The volcanic rocks from the top 320 m of the BOI are visually lower in $Fe^{3+}/\Sigma Fe$ than equivalent depths at Troodos, but the more oxidized Bay of Island volcanic rocks at depths of 390–650 m are similar to those at Troodos at an equivalent depth (Figures 5c and 5d).

Finally in Figures 5e and 5f, we compare our BOI data to volcanic rocks from various Deep Sea Drilling Project (and later iterations) drill cores of oceanic crust. Data are the same as those compiled in Stolper and Keller (2018) (n = 1,121 — note 30 samples from Stolper and Keller (2018) were not included as we could not calculate depths in terms of depth to sediment-basalt interface). We also include data from Site 504B, which is from Alt et al. (1996). The compiled data given in Stolper and Keller (2018) are only from oceanic crust older than 10 million years. This age cutoff was used to ensure most of the alteration that would occur on the seafloor has occurred in samples — previous work indicates that it takes at least 10 million years for most of the oxidation of the volcanic section to occur (Bach & Edwards, 2003; Johnson & Semyan, 1994). Igneous rocks from Site 504B are only 6 million years old. As such, the $Fe^{3+}/\Sigma Fe$ of the volcanic rocks may represent a minimum value as oxidative alteration may not yet be finished — for example, Alt et al. (1996) note that hydrothermal flow through the volcanic section is still occurring today. However, we include this system for comparison as it also has measurements of intrusive rocks.

The mean $Fe^{3+}/\Sigma Fe$ of cored >10 million year old marine volcanic rocks (as calculated in Stolper and Keller (2018)) is 0.41 (±0.01, 1 s.e.), which is elevated but within ±2 s.e. of the BOI volcanic samples. As discussed in Stolper and Keller (2018), the oceanic crust values are potentially biased due to incomplete recovery of the altered igneous rocks from cores. Corrections that take these potential sampling issues into account arrive at a mean $Fe^{3+}/\Sigma Fe$ for the volcanic section of oceanic crust of 0.56 (Staudigel et al., 1996) and thus similar to the values seen for the volcanic section at Macquarie Island (0.47) and Troodos (0.62). Based on this, we interpret the BOI volcanic $Fe^{3+}/\Sigma Fe$ to be lower than that of modern cored altered oceanic crust. This difference is also seen in the depth distribution. The three BOI volcanic rocks from the top 320 m of section are low in $Fe^{3+}/\Sigma Fe$ compared to typical Mesozoic and Cenozoic volcanic rocks from oceanic crust. However, the more oxidized volcanic rocks from BOI (390–650 m depth) overlap with oceanic volcanic rocks recovered from that depth range. We note that the cored samples compiled in Stolper and Keller (2018) are from systems where cores did not recover intrusive rocks and so a comparison to such rocks cannot be made.

Finally, Site 504B volcanic rocks yield a mean $Fe^{3+}/\Sigma Fe$ of 0.35 ± 0.006 (1 s.e., n = 157) versus 0.24 ± 0.003 (n = 261) in the intrusive section, equivalent to a difference of 0.11 ± 0.01 (1 s.e.). These rocks are thus more similar in $Fe^{3+}/\Sigma Fe$ to values we measured at BOI (0.29 for the volcanic rocks and 0.21 for the intrusive rocks with a difference of 0.09). However, as noted above, this system is sufficiently young that, if left for longer on the seafloor, $Fe^{3+}/\Sigma Fe$ of volcanic rocks would likely increase. Regardless, as was the case for the other ophiolites and drill cores, BOI volcanic rocks from the top 320 m are still not as oxidized at the site 504B volcanic rocks from a similar depth range, despite the latter likely not having seen its fully integrated history of oxidative alteration by low-temperature fluids.

5.2. Bay of Islands Versus Ophiolites From the Past 3.5 Billion Years

Here we compare the measured and compiled BOI data to a compilation of both extrusive and intrusive igneous rocks from other ophiolites formed over the past 3.5 billion years of Earth history. For the volcanic rocks, we use the already compiled data from Stolper and Keller (2018) and also include the Macquarie Island data and newly measured and compiled BOI data (which were not included in that work). This compilation did not include intrusive data and so, to address this, we newly compiled for this study intrusive data from the same ophiolites as those in Stolper and Keller (2018) (when intrusive data was available) and Macquarie Island. Specifically, we compiled 700 measurements of intrusive rocks from 36 localities (see Data Set S3 in Supporting Information S1) (724 points when the newly measured BOI data are included) — note that 73 ophiolites were included in the compilation of Stolper and Keller (2018), but not all had data for intrusive rocks.

To make this comparison, we bin data into the following time periods: the Precambrian (>541 Ma), Early Paleozoic (541–420 Ma), and Late Paleozoic-modern (<420 Ma). We note that in Stolper and Keller (2018) the Precambrian was further subdivided into time periods for the Archean, Paleo-Mesoproterozoic, and Neoproterozoic. They found no statistical differences between the various subdivisions for the Precambrian for volcanic rocks. As such, we combine them into one period. We additionally combine the Late Paleozoic (420–252 Ma) with the Mesozoic-Cenozoic (<252 Ma). These were also treated as separate in Stolper and Keller (2018) and did show differences in both mean and distributions $Fe^{3+}/\Sigma Fe$. We make these combinations as we are interested in differences between Early Paleozoic systems (like the BOI) versus older and younger rocks.

Histograms of $Fe^{3+}/\Sigma Fe$ are presented in Figure 6. Additionally, for the Late Paleozoic-modern systems, the Troodos ophiolite represents a significant amount of the compiled data (68% of the intrusive and 52% of the volcanic rocks). We show in Figure S2 in Supporting Information S1 that the volcanic and intrusive distributions for Troodos are similar to the equivalent distributions for the Late Paleozoic-modern without Troodos and thus that inclusion of the Troodos data does not obviously bias the shape of the histograms.

We now calculate and compare mean values for the different age ranges. To do this, we follow the approach of Stolper and Keller (2018) and calculate the mean $Fe^{3+}/\Sigma Fe$ of rocks of a specific type (volcanic or intrusive) from a given ophiolite and take the average of those means (only using ophiolites with at least two samples). This is done in order to avoid excess weighting of systems with more extensive sampling.

Although the focus here is on the BOI, we begin this comparison by looking at the Precambrian versus Late Paleozoic-Mesozoic in order to establish what the endmembers look like in a world generally thought to have had anoxic deep oceans (the Precambrian) versus a world thought to have oxygenated deep oceans (the Late Paleozoic-modern). Once we establish the differences between these systems (or lack thereof), we compare them to the BOI.

For the Precambrian, locality $Fe^{3+}/\Sigma Fe$ averages of the volcanic and intrusive rocks are 0.23 ± 0.01 (± 1 s.e., $n = 42$) and 0.22 (± 0.03, $n = 14$) respectively — note here n is the number of ophiolites. Thus, Precambrian intrusive and volcanic rocks are indistinguishable in terms of mean $Fe^{3+}/\Sigma Fe$. This overlap is also apparent in the $Fe^{3+}/\Sigma Fe$ distributions (Figures 6a and 6b) with peak values for both being between 0.1 and 0.3. The Precambrian contrasts with the Late Paleozoic to modern ophiolites where volcanic rocks yield a mean $Fe^{3+}/\Sigma Fe$ of 0.53 ± 0.04 (± 1 s.e., $n = 16$) versus 0.33 ± 0.04 ($n = 8$) for the intrusive rocks. Thus, unlike in the Precambrian, volcanic rocks from ophiolites are significantly (beyond $\pm$ 2 s.e.) more oxidized than the deeper crustal sections. These differences are also seen in the histograms (Figures 6g and 6h) in which the volcanic rocks are skewed to higher $Fe^{3+}/\Sigma Fe$ than the intrusive rocks and show a bimodal distribution. We interpret this bimodal distribution as follows: during oxidizing hydrothermal alteration, igneous rocks that are altered are generally moved from low $Fe^{3+}/\Sigma Fe$ (≈ 0.15) to high $Fe^{3+}/\Sigma Fe$ (>0.5) whereas those that are not altered are left with their original values. This can be understood to be the result of fluid flow through fracture systems in the volcanic section. Such unevenly distributed flow allows alteration to go to completion in the vicinity of the fracture (in this case oxidative alteration) but leaves distant mineral assemblages unaltered (Coogan & Gillis, 2018).

The elevation in $Fe^{3+}/\Sigma Fe$ of Late Paleozoic to modern volcanic ophiolitic rocks versus Precambrian equivalents was demonstrated in Stolper and Keller (2018) and interpreted to be due to the oxygenation of the deep ocean in the Phanerozoic, which then allowed for the delivery of O_2 to these rocks during low-temperature hydrothermal alteration. The addition of the intrusive rocks supports this interpretation. In the Precambrian no differences

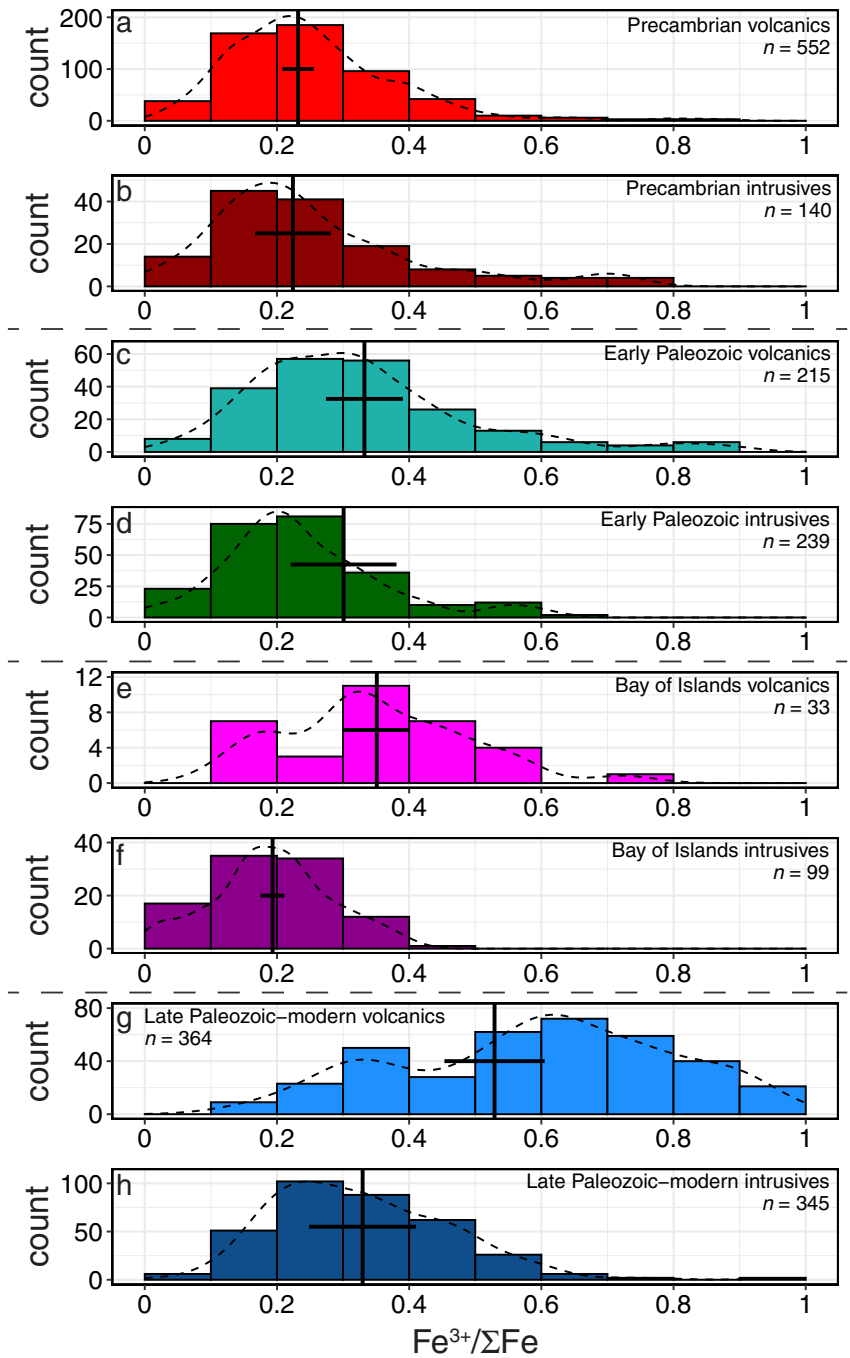

Figure 6. Comparison of $Fe^{3+}/\Sigma Fe$ from ophiolites of different ages. Solid black vertical lines are the mean values of each ophiolite for a specific time period (see main text), with horizontal 2 s.e. error bars. *n* is the number of data points. Dotted lines are smoothed distributions calculated using the default parameters of the stat_smooth function in the R statistical software package.

in $Fe^{3+}/\Sigma Fe$ between intrusive and extrusive rocks exist (and $Fe^{3+}/\Sigma Fe$ are low) while following 420 Ma $Fe^{3+}/\Sigma Fe$ of volcanic rocks is elevated versus intrusive rocks and shows a different distribution. That the Phanerozoic intrusive rocks are relatively less oxidized can be understood by the fact that the volcanic rocks see far more fluid (~100–1,000x) than deeper intrusive rocks (Coogan & Gillis, 2018; Elderfield & Schultz, 1996) and thus volcanic rocks will see a larger integrated flux of O_2 (if present in seawater) during their history on the seafloor. Although the intrusive rocks from <420 Ma are more oxidized on average than the Precambrian equivalents

(0.33 ± 0.04 versus 0.22 ± 0.03, 1 s.e.) these differences overlap at the ±2 s.e. level. However, the elevation $Fe^{3+}/\Sigma Fe$ between the Precambrian and <420 Ma rocks (Figure 6b vs. H) may also relate to changes in ocean chemistry. For example, such an elevation in Phanerozoic intrusive rocks could be due to the oxygenation of the deep ocean at this time if some dissolved O_2 reaches the intrusive rocks during hydrothermal alteration. Alternatively, such an increase may be related to changes in marine sulfate concentrations. Specifically, as discussed for the Troodos ophiolite, sulfate can oxidize iron at elevated (>200°C) temperatures (Shanks et al., 1981) and such temperatures characterize the hydrothermal alteration of intrusive rocks from oceanic crust. Marine sulfate concentrations have been proposed to have increased at the end of the Neoproterozoic (Algeo et al., 2015; Blättler et al., 2020; Kah et al., 2004) and, as such, this sulfate may have caused the oxidation of the deeper crustal sections in the Phanerozoic. Regardless, the intrusive data compiled here support the hypothesis of Stolper and Keller (2018) that significant increases in deep ocean O_2 concentrations from the Precambrian to Late Paleozoic changed the amount of oxidation occurring in the volcanic section while, as shown here, left the intrusive sections less disturbed in terms of the redox state of iron.

With the characteristics of these endmembers established, we now compare the Early Paleozoic data to them. We begin by examining all of the compiled and measured Late Paleozoic data before turning to the BOI specifically. The compilation of the Early Paleozoic (541–420 Ma) rocks (which includes BOI samples) yields a mean $Fe^{3+}/\Sigma Fe$ for the volcanic rocks of 0.33 ± 0.03 (1 s.e., $n = 15$) versus 0.30 ± 0.04 ($n = 11$) for the intrusive rocks. Thus, the two do not differ at the ±2 s.e. level. Additionally, the Early Paleozoic intrusive rocks do not differ from the Precambrian equivalents beyond 2 s.e. while the volcanic rocks do and are elevated in $Fe^{3+}/\Sigma Fe$ (0.33) versus the Precambrian (0.23). However, these differences in terms of the means are subtle. This is seen in the histograms where, for the intrusive rocks, the Precambrian and Early Paleozoic rocks are similar (peak in distributions of 0.2–0.3), while for the volcanic rocks, the Early Paleozoic rocks show a slight skew toward higher $Fe^{3+}/\Sigma Fe$ (peak distribution of 0.3–0.4 versus 0.2–0.3 in the Precambrian). The Early Paleozoic volcanic rocks do not show the bimodal distributions in $Fe^{3+}/\Sigma Fe$ seen in the more recent ophiolites. Thus, the Early Paleozoic $Fe^{3+}/\Sigma Fe$ distribution for volcanic rocks differs from the Late Paleozoic and younger rocks in two ways: (a) $Fe^{3+}/\Sigma Fe$ of Early Paleozoic volcanic rocks are typically lower than Late Paleozoic and younger rocks; And (b) the Early Paleozoic volcanic rocks do not show the bimodality in $Fe^{3+}/\Sigma Fe$ seen in in the Late Paleozoic and younger rocks.

Unlike for the compilation that includes all ophiolites, the Early Paleozoic BOI volcanic and intrusive rocks are, on average, measurably different in $Fe^{3+}/\Sigma Fe$: 0.35 ± 0.02 (±1 s.e., $n = 33$) versus 0.19 ± 0.01 ($n = 99$). The volcanic value is indistinguishable at ±2 s.e., from the mean Early Paleozoic rocks for all ophiolites examined (0.33 ± 0.02), while the intrusive rocks are lower (0.19 ± 0.01 vs. 0.30 ± 0.04) and more similar to the Precambrian values (0.22 ± 0.03). The histograms also show this difference with BOI volcanic rocks $Fe^{3+}/\Sigma Fe$ skewed to higher values (most >0.3) compared to the intrusive rocks and the compilation of Early Paleozoic and Precambrian values. However, this oxidation is significantly less both in mean and peak distribution compared to the Late Paleozoic-modern examples. For example, in Late Paleozoic-modern ophiolites, most volcanic $Fe^{3+}/\Sigma Fe$ are >0.6 (53% of the data), whereas such elevated values are rare for BOI (3% of the data). This indicates that for BOI: (*i*) oxidation in the volcanic rocks does seem to have occurred preferentially relative to the intrusive section; But (*ii*) the oxidation in the volcanic rocks occurred to less of an extent as is generally seen in the Late Paleozoic-modern systems.

6. Discussion

6.1. Bay of Islands $Fe^{3+}/\Sigma Fe$

The question motivating this study is whether or not the hydrothermal alteration of BOI igneous rocks was associated with oxidative alteration by O_2 and if so, to what degree. Based on the results described above, BOI samples show some degree of elevation in $Fe^{3+}/\Sigma Fe$ in the volcanic rocks versus the intrusive sections — when all BOI data are combined (measured here and compiled), we observe that the mean Paleozoic BOI volcanic and intrusive rocks are, on average, measurably different in $Fe^{3+}/\Sigma Fe$: 0.35 ± 0.02 (±1 s.e., $n = 33$) versus 0.19 ± 0.01 ($n = 99$). The volcanic values are elevated compared to Precambrian volcanic and intrusive $Fe^{3+}/\Sigma Fe$ averages: 0.23 ± 0.01 (±1 s.e., $n = 42$) and 0.22 (±0.03, $n = 14$. Both are lower than values seen in the Late Paleozoic to modern, with a mean for volcanic rocks of 0.53 ± 0.04 (±1 s.e., $n = 16$) versus 0.33 ± 0.04 ($n = 8$) for the intrusive rocks.

Thus, as compared to the Precambrian, the BOI volcanic samples are somewhat oxidized, but both share similar values for the intrusive sections. We propose that this elevated oxidation in the BOI volcanic section is not due to later metamorphism (e.g., during obduction) or during subaerial exposure, but instead occurred while in place on the seafloor by oxidizing hydrothermal fluids. Our basis in stating this is that we would expect that if such later oxidation had occurred, it would have affected the volcanic rocks and intrusive rocks equally as opposed to being concentrated in the extrusive rocks. As such, we propose that the volcanic rocks show evidence for some degree of oxidation by O_2 during seawater alteration and thus provide evidence for the presence of O_2 in the water masses that fed the hydrothermal systems in the BOI formational environment.

We note that this differs from the proposal of Stolper and Keller (2018). Specifically, they proposed that it was 'probably' not until the Late Paleozoic that O_2 concentrations reached sufficient levels to clearly oxidize volcanic rocks — that is, there may be a shift in the Early Paleozoic in terms of volcanic $Fe^{3+}/\Sigma Fe$, but it is not until the Late Paleozoic-Modern that this shift is readily apparent. This proposal was based on the general similarity of $Fe^{3+}/\Sigma Fe$ in the Early Paleozoic and Precambrian volcanic rocks and differences between Early Paleozoic and younger rocks (Figure 6).

If our interpretation of the BOI data set is correct, it would indicate that this prior interpretation based on the compiled data, though apparently supported when looking at time-bin averages, is not the complete story. Instead, by focusing on a specific location, that at least for this specific system, O_2 was present in the source waters feeding the hydrothermal systems in the Late Paleozoic.

However, it also appears that these O_2 levels were less than what was typical during hydrothermal alteration of ophiolites from the Late Paleozoic to today. This is observed both in the mean values discussed above and in the depth distributions of $Fe^{3+}/\Sigma Fe$. Specifically, the comparison of the BOI data measured as a function depth versus the Troodos and Macquarie Island as well as drilled oceanic crust indicates that the BOI samples do not show the same degree of iron oxidation as these younger systems (Figure 5). Volcanic rocks from above 320 m and below 720 m have $Fe^{3+}/\Sigma Fe$ of 0.1–0.2 and thus scatter around the values expected for modern MORB. We can rule out for the shallowest samples (<320 m) that no hydrothermal alteration occurred as these samples have elevated K_2O contents, which is indicative of low-temperature hydrothermal alteration (Figure 3). As such, for these samples, we interpret that the lower $Fe^{3+}/\Sigma Fe$ are due to alteration in fluids that contained less O_2 as compared to younger ophiolites. Although K_2O levels are generally within the range expected for unaltered igneous rocks below this depth (320 m), both potassium isotopes (Parendo et al., 2017) and strontium isotopes (Jacobsen & Wasserburg, 1979) indicate that hydrothermal alteration of seawater occurred down to the gabbroic section — note that these studies were on rocks from the Blow-Me-Down Massif (as opposed to the North Arm Mountain massif studied here). Regardless, we expect that hydrothermal fluids penetrated to the gabbros for the samples measured here as well. Additionally, we note that the volcanic samples with elevated $Fe^{3+}/\Sigma Fe$ (>0.4) do not show enhancements in K_2O content (<0.25 wt. %) indicating that oxidation of these rocks did not co-occur with extensive potassium uptake. This is not unusual in modern marine hydrothermal systems: in a cross plot of $Fe^{3+}/\Sigma Fe$ versus K_2O, the volcanic rocks at BOI with elevated $Fe^{3+}/\Sigma Fe$ but low K_2O contents overlap data for volcanic rocks from Site 504B, Troodos, and other BOI samples (Figure S3 in Supporting Information S1).

In contrast, the samples from 390 to 650 m depth yield elevated $Fe^{3+}/\Sigma Fe$: 0.41–0.51. We interpret the grouping of elevated volcanic $Fe^{3+}/\Sigma Fe$ over 250 m of depth to indicate that the flow of oxidizing fluids was focused over this depth interval, whereas fluids that flowed above and below this section were not sufficiently oxidizing to measurably increase volcanic $Fe^{3+}/\Sigma Fe$. Put another way, we propose that fluids that altered the measured volcanic rocks above 390 m and below 650 m were anoxic while those between 390 and 650 m contained some dissolved O_2 during low temperature alteration that oxidized the iron.

A question is why, if this interpretation is correct, is the oxidation apparently focused in the middle of the volcanic section as opposed to throughout or the top of the section which, in general, sees more fluid flow than deeper sections (Coogan & Gillis, 2018)? We propose the following explanation: during hydrothermal flow through the volcanic section, water enters and exits the system at different points and flows along fractures. As that water flows, O_2 dissolved in the water can react with and oxidize igneous minerals adjacent to the fracture. However, if all of the O_2 in fluid is consumed before it exits the hydrothermal system back to the ocean, rocks altered at the end of the flow path will instead react in anoxic fluids and thus not become oxidized despite being hydrothermally altered. Thus it is the combination of the integrated water flux, concentration of O_2 in the starting fluid, and

proximity to the inlet of seawater to the volcanic aquifer that controls the amount of oxidation at a given position in the volcanic section. An explanation for the observed oxidation in the mid-depth volcanic section samples is that they happened to have been closer to a fluid entrance point into the volcanic aquifers versus the other samples and thus, during alteration, the fluid still had O_2 present versus the other samples that were altered in fluids that had gone anoxic earlier in the flow path. This is consistent with the oxidized samples (4, 5, 6, and 7 in Figure 1), all being collected in the same vicinity.

Based on the above discussion, we propose that the BOI volcanic section did experience alteration in oxidizing conditions and that this was done by O_2 dissolved in seawater. This is distinct from the Precambrian equivalents that do not show evidence for this. However, the degree of oxidation appears less than what is typical in volcanic rocks from the Late Paleozoic to modern indicating that O_2 concentrations were, on average, lower in the seawater that fed the hydrothermal systems of the BOI as compared to typical Late Paleozoic and younger equivalents.

We now attempt to quantify the oxygen concentration in the waters that altered the BOI rocks. We do this following the approach outlined in Stolper and Keller (2018), which calculates the amount of O_2 needed to increase the $Fe^{3+}/\Sigma Fe$ of the volcanic section above the initial value. The methods and assumptions are stated in that study. Here we assume the starting $Fe^{3+}/\Sigma Fe$ of the volcanic rocks is the mean of the intrsuive section (0.19 ± 0.01, 1 s.e.) and that they are oxidized to the mean of the volcanic section (0.35 ± 0.02). Using the same model assumptions as in Stolper and Keller (2018) yields a deep ocean concentration of 34 ± 16 μmol O_2/kg seawater (1σ), which is 2.4× lower than that calculated for the Mesozoic and Cenozoic deep oceans by Stolper and Keller (2018).

6.2. Implications of the Bay of Islands for Early Paleozoic Deep-Ocean O_2 Concentrations

Based on the above discussion, we interpret the $Fe^{3+}/\Sigma Fe$ of the BOI to indicate that the seawater that altered the BOI volcanic rocks contained some dissolved O_2, but that this concentration was lower than calculated previously for Mesozoic and Cenozoic O_2 concentrations. The question we take up here is what bearing this has on the history of deep-ocean O_2 concentrations.

Our discussion of the history of deep-ocean O_2 above has implicitly followed a simplifying conceptual framework introduced by others (e.g., Canfield, 1998; Laakso & Schrag, 2014; Lyons et al., 2014; Sarmiento et al., 1988) in which the ocean is effectively separated into various boxes that includes, at a minimum, (*i*) a shallow box in contact with the atmosphere with O_2 concentrations in equilibrium with atmospheric O_2 and (*ii*) a deeper box that is not in contact with the atmosphere and whose O_2 is set by the downwelling water from the shallower box(es) into the deep box and the amount of respiration in the deep ocean box. In this framework, there is effectively one deep-ocean O_2 concentration. However, in the modern world, O_2 concentrations vary both in and between ocean basins as a function of water mass age, source region, and overlying biological productivity. For example, deep water (>2,000 m) in the Atlantic versus the Pacific can differ by ∼100 μmol/kg seawater as compared to the average deep-ocean O_2 concentration of ∼180 μmol/kg seawater (Sarmiento & Gruber, 2006). Additionally, marine water masses can go anoxic at some depths (so-called oxygen minimum zones). We raise this because, ultimately, the O_2 concentrations in the water masses that fed the hydrothermal systems of the BOI igneous rocks are fundamentally local and likely different from any hypothetical mean deep-ocean O_2 concentration that existed at this time.

As discussed in Section 2, the BOI igneous rocks formed in the Iapetus Ocean. Although paleoceanographic constrains are limited, based on sediments intercalated in the pillow basalts (radiolarian cherts), the formational environment appears to have been a deep-water open-ocean setting. The lack of terrigenous sediment also suggests formation in an open ocean setting. Typical water depths for modern mid-ocean ridges are generally >2,000 m. Similar water depths are observed for spreading systems associated with subduction-zone settings such as back-arc basins (e.g., Taylor & Martinez, 2003). Today, these depths are below typical modern oxygen minimum zone depths and are at depths typically taken to represent deep water masses sourced from high latitudes that represent the majority of the ocean's volume (Sarmiento & Gruber, 2006). Given this, we assume that the source of fluids to the BOI hydrothermal systems was below the wind mixed layer and likely below any potential local oxygen minimum zones. On this basis, we assume the fluid sources approximate average deep-ocean water chemistry in the Iapetus Ocean.

As such, we propose that some deep-water masses in the Early Paleozoic did have sufficient O_2 (order tens of micromoles/kg seawater) to cause some oxidation of basalts during hydrothermal circulation. However, this oxygen concentration was less than that of the Later Paleozoic, Mesozoic, and Cenozoic. A question is if this condition was common throughout the Early Paleozoic both in time and space? The BOI data cannot answer this as it is in a specific location. However, in looking at the data available for Early Paleozoic rocks, the BOI does not stand out as particularly distinct. Its mean value for the $Fe^{3+}/\Sigma Fe$ of the volcanic rocks (0.35) is similar to the mean for all 15 localities (0.33), which span an age range of 530 to 440 million years. Additionally, the histograms indicate that although the Late Paleozoic volcanic rocks show some small degree of iron oxidation compared to Precambrian equivalents, higher degrees of oxidation do not occur until after the Late Paleozoic.

On this basis, we propose that in the Early Paleozoic (~485 million years ago) there were moderate amounts of O_2 in the deep ocean, but at concentrations significantly lower than found today. This oxygen was able to oxidize portions of the volcanic section of the BOI ophiolite, but not to the levels seen after the Late Paleozoic and that it was not until this later time frame that deep-ocean O_2 concentrations were sufficient for clear and significant oxidation of marine volcanic rocks during low-temperature hydrothermal alteration. An explanation for these changes is that any increases in O_2 concentrations that did occur in the late Neoproterozoic to Early Paleozoic above previously lower values in the Proterozoic were insufficient to oxygenate the deep ocean to modern levels and were then followed by an additional increase in O_2 levels to near modern levels in the Late Paleozoic. This interpretation is broadly consistent with a variety of recent studies on the evolution of atmospheric and marine O_2 concentrations from the Proterozoic to Phanerozoic (see review in Tostevin & Mills, 2020). However, other explanations including changes in O_2 solubility (due to temperature changes), ocean circulation, and/or biological productivity are also possible as these also control deep-ocean oxygen concentrations.

Finally, the calculated O_2 concentrations in the deep ocean based on the BOI volcanic versus intrusive data are sufficiently low that small changes in either atmospheric O_2 concentrations or oceanographic conditions (e.g., solubility of O_2 due to temperature changes, circulation changes, and/or the strength of the biological pump) could have driven parts of the ocean to anoxia more readily than can occur today. Such could allow for more oscillations in the redox chemistry of the deep ocean in time and space. This supports the proposal for variable O_2 contents of Paleozoic marine waters with swings toward higher and lower O_2 concentration over relatively short time periods (e.g., order millions of years), sometimes termed ocean oxygenation events (e.g., Kendall et al., 2015; Reinhard & Planavsky, 2022; Sahoo et al., 2016; Tostevin & Mills, 2020). Such oscillations would also explain why, when all Early Paleozoic $Fe^{3+}/\Sigma Fe$ of volcanic rocks from ophiolites are combined into one bin, they are not as obviously oxidized versus their Precambrian counterparts as compared to Late Paleozoic and younger rocks. This may be because some are indeed not oxidized, that is, they formed in a region of the ocean or time in the Early Paleozoic when the deep ocean was anoxic. In conrast, others may have formed and been altered by waters with finite but low O_2 concentrations (<50 μmol O_2/kg seawater). This could be tested by conducting a similar study as this on a range of Early Paleozoic ophiolites looking at $Fe^{3+}/\Sigma Fe$ of both intrusive and extrusive rocks.

7. Summary and Conclusions

This study shows that for the BOI ophiolite, $Fe^{3+}/\Sigma Fe$ values of the volcanic section are elevated compared to Precambrian ophiolites, but lower than those of the Late Paleozoic to modern. The BOI intrusive section does not show this elevation. These differences are seen both via comparisons of $Fe^{3+}/\Sigma Fe$ as a function of depth in the BOI versus Mesozoic and Cenozoic Ophiolites and oceanic crust as well as in a comparison to a larger data compilation of $Fe^{3+}/\Sigma Fe$ values for volcanic and intrusive rocks from ophiolites ranging in age from the Archean to Cenozoic. Based on this, we propose that the BOI volcanic section was altered at low temperatures in fluids that contained some, but lower (~2.4×) O_2 concentrations as compared to today. Thus, the Early Paleozoic, at least at the time of the BOI formation (485 Ma), was a time of low, but not negligible oxygen concentrations in the deep ocean. These O_2 concentrations may have been sufficiently low to allow for the deep ocean to be spatially heterogenous in terms of O_2 concentration (e.g., anoxic in some places but oxic in others) as well as to oscillate between oxygenated and anoxic conditions on relatively short geologic timescales (e.g., order millions of years). The data also support previous work that proposed that it was not until the Late Paleozoic (~420 Ma) that the deep ocean appears to have become persistently oxygenated.

Data Availability Statement

The newly produced and compiled data for this paper are contained in the text, figures and Supporting Information and are also archived externally at https://doi.org/10.5281/zenodo.6262559. Data associated with Stolper and Keller (2018) are available from https://doi.org/10.1038/nature25009.

Acknowledgments
DAS acknowledges support from an Esper Larsen Jr. Research Grant. MKL acknowledges support from the Agouron Institute Geobiology Postdoctoral Fellowship. XP and RAL acknowledge support from University of Michigan discretionary research funds. DAS thanks N Swanson-Hysell for helpful discussions on the paleogeography of Early Paleozoic landmasses.

References

Alcott, L. J., Mills, B. J., & Poulton, S. W. (2019). Stepwise Earth oxygenation is an inherent property of global biogeochemical cycling. *Science*, *366*(6471), 1333–1337. https://doi.org/10.1126/science.aax6459

Algeo, T. J., Luo, G. M., Song, H. Y., Lyons, T. W., & Canfield, D. E. (2015). Reconstruction of secular variation in seawater sulfate concentrations. *Biogeosciences*, *12*(7), 2131–2151. https://doi.org/10.5194/bg-12-2131-2015

Alt, J. C., Laverne, C., Vanko, D. A., Tartarotti, P., Teagle, D. A., Bach, W., et al. (1996). Hydrothermal alteration of a section of upper oceanic crust in the eastern equatorial Pacific: A synthesis of results from site 504 (DSDP legs 69, 70, and 83, and ODP legs 111, 137, 140, and 148). *Proceedings of the Ocean Drilling Program, Scientific Results*, *148*, 417–434.

Archibald, D. A., & Farrar, E. (1976). K–Ar ages of amphiboles from the Bay of Islands ophiolite and the Little Port Complex, Western Newfoundland, and their geological implications. *Canadian Journal of Earth Sciences*, *13*(4), 520–529. https://doi.org/10.1139/e76-055

Bach, W., & Edwards, K. J. (2003). Iron and sulfide oxidation within the basaltic ocean crust: Implications for chemolithoautotrophic microbial biomass production. *Geochimica et Cosmochimica Acta*, *67*(20), 3871–3887. https://doi.org/10.1016/S0016-7037(03)00304-1

Blamey, N. J., Brand, U., Parnell, J., Spear, N., Lécuyer, C., Benison, K., et al. (2016). Paradigm shift in determining Neoproterozoic atmospheric oxygen. *Geology*, *44*(8), 651–654. https://doi.org/10.1130/G37937.1

Blättler, C. L., Bergmann, K. D., Kah, L. C., Gómez-Pérez, I., & Higgins, J. A. (2020). Constraints on Meso-to Neoproterozoic seawater from ancient evaporite deposits. *Earth and Planetary Science Letters*, *532*, 115951. https://doi.org/10.1016/j.epsl.2019.115951

Brounce, M., Kelley, K. A., Cottrell, E., & Reagan, M. K. (2015). Temporal evolution of mantle wedge oxygen fugacity during subduction initiation. *Geology*, *43*(9), 775–778. https://doi.org/10.1130/G36742.1

Brounce, M. N., Kelley, K., & Cottrell, E. (2014). Variations in $Fe^{3+}/\Sigma Fe$ of Mariana arc basalts and mantle wedge fO_2. *Journal of Petrology*, *55*(12), 2513–2536. https://doi.org/10.1093/petrology/egu065

Bucholz, C. E., & Spencer, C. J. (2019). Strongly peraluminous granites across the Archean–Proterozoic transition. *Journal of Petrology*, *60*(7), 1299–1348. https://doi.org/10.1093/petrology/egz033

Canfield, D. E. (1998). A new model for Proterozoic ocean chemistry. *Nature*, *396*(6710), 450–453. https://doi.org/10.1038/24839

Canfield, D. E. (2005). The early history of atmospheric oxygen: Homage to Robert M. Garrels. *Annual Review of Earth and Planetary Sciences*, *33*, 1–36. https://doi.org/10.1146/annurev.earth.33.092203.122711

Casey, J. F., Dewey, J. F., Fox, P. J., Karson, J. A., & Rosencrantz, E. (1981). Heterogeneous nature of the oceanic crust and upper mantle: A perspective from the Bay of Islands Ophiolite. In C. Emiliani (Ed.), *The Sea* (Vol. *7*, pp. 305–338). Wiley.

Casey, J. F., Elthon, D. L., Siroky, F. X., Karson, J. A., & Sullivan, J. (1985). Geochemical and geological evidence bearing on the origin of the Bay of islands and coastal complex ophiolites of Western Newfoundland. *Tectonophysics*, *116*(1–2), 1–40. https://doi.org/10.1016/0040-1951(85)90220-3

Casey, J. F., & Kidd, W. S. F. (1981). A parallochthonous group of sedimentary rocks unconformable overlying the Bay of Islands ophiolite complex, North Arm Mountain, Newfoundland. *Canadian Journal of Earth Sciences*, *18*(6), 1035–1050. https://doi.org/10.1139/e81-100

Cawood, P. A., & Suhr, G. (1992). Generation and obduction of ophiolites: Constraints from the Bay of islands complex, Western Newfoundland. *Tectonics*, *11*(4), 884–897. https://doi.org/10.1029/92TC00471

Christensen, N. I., & Salisbury, M. H. (1982). Lateral heterogeneity in the seismic structure of the oceanic crust inferred from velocity studies in the Bay of Islands ophiolite, Newfoundland. *Geophysical Journal International*, *68*(3), 675–688. https://doi.org/10.1111/j.1365-246X.1982.tb04922.x

Church, W. T., & Stevens, R. K. (1971). Early Paleozoic ophiolite complexes of the Newfoundland Appalachians as mantle-oceanic crust sequences. *Journal of Geophysical Research*, *76*(5), 1460–1466. https://doi.org/10.1029/JB076i005p01460

Coggon, R. M. (2006). *Hydrothermal alteration of the ocean crust: Insights from Macquarie island and drilled in situ ocean crust* (PhD thesis). University of Southampton.

Coggon, R. M., Teagle, D. A., Harris, M., Davidson, G. J., Alt, J. C., & Brewer, T. S. (2016). Hydrothermal contributions to global biogeochemical cycles: Insights from the Macquarie Island ophiolite. *Lithos*, *264*, 329–347. https://doi.org/10.1016/j.lithos.2016.08.024

Coish, R. A. (1977). *Igneous and metamorphic petrology of the mafic units of the Betts Cove and Blow-Me-Down ophiolites* (PhD thesis). The University of Western Ontario.

Coogan, L. A., & Gillis, K. M. (2018). Low-temperature alteration of the seafloor: Impacts on ocean chemistry. *Annual Review of Earth and Planetary Sciences*, *46*(1), 21–45. https://doi.org/10.1146/annurev-earth-082517-010027

Coogan, L. A., Parrish, R. R., & Roberts, N. M. (2016). Early hydrothermal carbon uptake by the upper oceanic crust: Insight from in situ U-Pb dating. *Geology*, *44*(2), 147–150. https://doi.org/10.1130/G37212.1

Cottrell, E., & Kelley, K. A. (2011). The oxidation state of Fe in MORB glasses and the oxygen fugacity of the upper mantle. *Earth and Planetary Science Letters*, *305*(3), 270–282. https://doi.org/10.1016/j.epsl.2011.03.014

Dahl, T. W., Hammarlund, E. U., Anbar, A. D., Bond, D. P., Gill, B. C., Gordon, G. W., et al. (2010). Devonian rise in atmospheric oxygen correlated to the radiations of terrestrial plants and large predatory fish. *Proceedings of the National Academy of Sciences*, *107*(42), 17911–17915. https://doi.org/10.1073/pnas.1011287107

Dallmeyer, R. D., & Williams, H. (1975). $^{40}Ar/^{39}Ar$ ages from the Bay of islands metamorphic aureole: Their bearing on the timing of ordovician ophiolite obduction. *Canadian Journal of Earth Sciences*, *12*(9), 1685–1690. https://doi.org/10.1139/e75-148

Dewey, J. F., & Casey, J. F. (2013). The sole of an ophiolite: The ordovician Bay of islands complex, Newfoundland. *Journal of the Geological Society*, *170*(5), 715–722. https://doi.org/10.1144/jgs2013-017

Duke, N. A., & Hutchinson, R. W. (1974). Geological relationships between massive sulfide bodies and ophiolitic volcanic rocks near York Harbour, Newfoundland. *Canadian Journal of Earth Sciences*, *11*(1), 53–69. https://doi.org/10.1139/e74-005

Dunning, G., & Krogh, T. (1985). Geochronology of ophiolites of the Newfoundland appalachians. *Canadian Journal of Earth Sciences*, *22*(11), 1659–1670. https://doi.org/10.1139/e85-174

Elderfield, H., & Schultz, A. (1996). Mid-ocean ridge hydrothermal fluxes and the chemical composition of the ocean. *Annual Review of Earth and Planetary Sciences*, *24*(1), 191–224. https://doi.org/10.1146/annurev.earth.24.1.191

Elthon, D. (1991). Geochemical evidence for formation of the Bay of Islands ophiolite above a subduction zone. *Nature*, *354*(6349), 140–143. https://doi.org/10.1038/354140a0

Evans, K. A. (2012). The redox budget of subduction zones. *Earth-Science Reviews*, *113*(1–2), 11–32. https://doi.org/10.1016/j.earscirev.2012.03.003

Farquhar, J., Bao, H., & Thiemens, M. (2000). Atmospheric influence of Earth's earliest sulfur cycle. *Science*, *289*(5480), 756–758. https://doi.org/10.1126/science.289.5480.756

Fitton, J. G., & Gill, R. C. O. (1970). The oxidation of ferrous iron in rocks during mechanical grinding. *Geochimica et Cosmochimica Acta*, *34*(4), 518–524. https://doi.org/10.1016/0016-7037(70)90143-2

Gale, A., Dalton, C. A., Langmuir, C. H., Su, Y., & Schilling, J. (2013). The mean composition of ocean ridge basalts. *Geochemistry, Geophysics, Geosystems*, *14*(3), 489–518. https://doi.org/10.1029/2012GC004334

Gibson, I. L., Malpas, J., Robinson, P. T., & Xenophontos, C. (Eds.) (1989). *Cyprus crustal study project: Initial report, hole CY-4*, *Geological Survey of Canada paper*. 88-9.

Gibson, I. L., Malpas, J., Robinson, P. T., & Xenophontos, C. (Eds.) (1991). *Cyprus crustal study project: Initial report, holes Cy-1 and 1a*, *Geological Survey of Canada paper*. 90-20.

Hart, S. R., & Staudigel, H. (1978). Oceanic crust: Age of hydrothermal alteration. *Geophysical Research Letters*, *5*(12), 1009–1012. https://doi.org/10.1029/GL005i012p01009

Hart, S. R., & Staudigel, H. (1982). The control of alkalies and uranium in seawater by ocean crust alteration. *Earth and Planetary Science Letters*, *58*(2), 202–212. https://doi.org/10.1016/0012-821X(82)90194-7

Jacobsen, S. B., & Wasserburg, G. J. (1979). Nd and Sr isotopic study of the Bay of Islands ophiolite complex and the evolution of the source of midocean ridge basalts. *Journal of Geophysical Research*, *84*(B13), 7429–7445. https://doi.org/10.1029/JB084iB13p07429

Jenner, G., Dunning, G., Malpas, J., Brown, M., & Brace, T. (1991). Bay of islands and little port complexes, revisited: Age, geochemical and isotopic evidence confirm suprasubduction-zone origin. *Canadian Journal of Earth Sciences*, *28*(10), 1635–1652. https://doi.org/10.1139/e91-146

Johnson, H. P., & Semyan, S. W. (1994). Age variation in the physical properties of oceanic basalts: Implications for crustal formation and evolution. *Journal of Geophysical Research*, *99*(B2), 3123–3134. https://doi.org/10.1029/93JB00717

Kah, L. C., Lyons, T. W., & Frank, T. D. (2004). Low marine sulphate and protracted oxygenation of the Proterozoic biosphere. *Nature*, *431*(7010), 834–838. https://doi.org/10.1038/nature0297

Kelley, K. A., Plank, T., Ludden, J., & Staudigel, H. (2003). Composition of altered oceanic crust at ODP Sites 801 and 1149. *Geochemistry, Geophysics, Geosystems*, *4*(6). https://doi.org/10.1029/2002GC000435

Kendall, B., Komiya, T., Lyons, T. W., Bates, S. M., Gordon, G. W., Romaniello, S. J., et al. (2015). Uranium and molybdenum isotope evidence for an episode of widespread ocean oxygenation during the late Ediacaran Period. *Geochimica et Cosmochimica Acta*, *156*, 173–193. https://doi.org/10.1016/j.gca.2015.02.025

Laakso, T. A., & Schrag, D. P. (2014). Regulation of atmospheric oxygen during the Proterozoic. *Earth and Planetary Science Letters*, *388*, 81–91. https://doi.org/10.1016/j.epsl.2013.11.049

Lenton, T. M., Dahl, T. W., Daines, S. J., Mills, B. J., Ozaki, K., Saltzman, M. R., & Porada, P. (2016). Earliest land plants created modern levels of atmospheric oxygen. *Proceedings of the National Academy of Sciences*, *113*(35), 9704–9709. https://doi.org/10.1073/pnas.1604787113

Lyons, T. W., Reinhard, C. T., & Planavsky, N. J. (2014). The rise of oxygen in Earth's early ocean and atmosphere. *Nature*, *506*(7488), 307–315. https://doi.org/10.1038/nature13068

Mac Niocaill, C., Van der Pluijm, B. A., & Van der Voo, R. (1997). Ordovician paleogeography and the evolution of the Iapetus Ocean. *Geology*, *25*(2), 159–162. https://doi.org/10.1130/0091-7613(1997)025%3C0159:OPATEO%3E2.3.CO;2

Malpas, J. (1976). *The petrology and petrogenesis of the Bay of Islands ophiolite suite, western Newfoundland* (PhD thesis). Memorial University of Newfoundland.

Malpas, J. (1977). Petrology and tectonic significance of Newfoundland ophiolites, with examples from the Bay of Islands. In *North American ophiolites* (Vol. 95, pp. 13–23). State of Oregon Department of Geology and Mineral Resources.

Neal, C., & Stanger, G. (1983). Hydrogen generation from mantle source rocks in Oman. *Earth and Planetary Science Letters*, *66*, 315–320. https://doi.org/10.1016/0012-821X(83)90144-9

Och, L. M., & Shields-Zhou, G. A. (2012). The neoproterozoic oxygenation event: Environmental perturbations and biogeochemical cycling. *Earth-Science Reviews*, *110*(1), 26–57. https://doi.org/10.1016/j.earscirev.2011.09.004

Osozawa, S., Shinjo, R., Lo, C.-H., Jahn, B., Hoang, N., Sasaki, M., et al. (2012). Geochemistry and geochronology of the Troodos ophiolite: An SSZ ophiolite generated by subduction initiation and an extended episode of ridge subduction? *Lithosphere*, *4*(6), 497–510. https://doi.org/10.1130/L205.1

Parendo, C. A., Jacobsen, S. B., & Wang, K. (2017). K isotopes as a tracer of seafloor hydrothermal alteration. *Proceedings of the National Academy of Sciences*, *114*(8), 1827–1831. https://doi.org/10.1073/pnas.1609228114

Pavlov, A., & Kasting, J. (2002). Mass-independent fractionation of sulfur isotopes in archean sediments: Strong evidence for an anoxic archean atmosphere. *Astrobiology*, *2*(1), 27–41. https://doi.org/10.1089/153110702753621321

Planavsky, N. J., Cole, D. B., Isson, T. T., Reinhard, C. T., Crockford, P. W., Sheldon, N. D., & Lyons, T. W. (2018). A case for low atmospheric oxygen levels during Earth's middle history. *Emerging Topics in Life Sciences*, *2*(2), 149–159. https://doi.org/10.1042/ETLS20170161

Planavsky, N. J., Robbins, L. J., Kamber, B. S., & Schoenberg, R. (2020). Weathering, alteration and reconstructing Earth's oxygenation. *Interface Focus*, *10*(4), 20190140. https://doi.org/10.1098/rsfs.2019.0140

Reinhard, C. T., & Planavsky, N. J. (2022). The history of ocean oxygenation. *Annual Review of Marine Science*, *14*(1), 331–353. https://doi.org/10.1146/annurev-marine-031721-104005

Richards, J. P. (2015). The oxidation state, and sulfur and Cu contents of arc magmas: Implications for metallogeny. *Lithos*, *233*, 27–45. https://doi.org/10.1016/j.lithos.2014.12.011

Robinson, P. T., Gibson, I. L., & Panayiotou, A. (Eds.) (1987). *Cyprus crustal study project: Initial report, holes CY-2 and 2a*, *Geological Survey of Canada paper*. 85-29.

Rutter, J. (2015). *Characterising low temperature alteration and oxidation of the upper oceanic crust* (PhD thesis). University of Southampton.

Sahoo, S. K., Planavsky, N. J., Jiang, G., Kendall, B., Owens, J. D., Wang, X., et al. (2016). Oceanic oxygenation events in the anoxic Ediacaran Ocean. *Geobiology*, *14*(5), 457–468. https://doi.org/10.1111/gbi.12182

Sahoo, S. K., Planavsky, N. J., Kendall, B., Wang, X., Shi, X., Scott, C., et al. (2012). Ocean oxygenation in the wake of the Marinoan glaciation. *Nature*, *489*(7417), 546–549. https://doi.org/10.1038/nature11445

Sarmiento, J. L., & Gruber, N. (2006). *Ocean biogeochemical dynamics*. Princeton University Press.
Sarmiento, J. L., Herbert, T. D., & Toggweiler, J. R. (1988). Causes of anoxia in the world ocean. *Global Biogeochemical Cycles*, *2*(2), 115–128. https://doi.org/10.1029/GB002i002p00115
Shanks, W. C., III, Bischoff, J. L., & Rosenbauer, R. J. (1981). Seawater sulfate reduction and sulfur isotope fractionation in basaltic systems: Interaction of seawater with fayalite and magnetite at 200–350 C. *Geochimica et Cosmochimica Acta*, *45*(11), 1977–1995. https://doi.org/10.1016/0016-7037(81)90054-5
Slotznick, S. P., Eiler, J. M., & Fischer, W. W. (2018). The effects of metamorphism on iron mineralogy and the iron speciation redox proxy. *Geochimica et Cosmochimica Acta*, *224*, 96–115. https://doi.org/10.1016/j.gca.2017.12.003
Slotznick, S. P., Webb, S. M., Kirschvink, J. L., & Fischer, W. W. (2019). Mid-Proterozoic ferruginous conditions reflect postdepositional processes. *Geophysical Research Letters*, *46*(6), 3114–3123. https://doi.org/10.1029/2018GL081496
Sperling, E. A., Melchin, M. J., Fraser, T., Stockey, R. G., Farrell, U. C., Bhajan, L., et al. (2021). A long-term record of early to mid-Paleozoic marine redox change. *Science Advances*, *7*(28), eabf4382. https://doi.org/10.1126/sciadv.abf4382
Sperling, E. A., Wolock, C. J., Morgan, A. S., Gill, B. C., Kunzmann, M., Halverson, G. P., et al. (2015). Statistical analysis of iron geochemical data suggests limited late Proterozoic oxygenation. *Nature*, *523*(7561), 451–454. https://doi.org/10.1038/nature14589
Staudigel, H., Plank, T., White, B., & Schmincke, H. (1996). Geochemical fluxes during seafloor alteration of the basaltic upper oceanic crust: DSDP sites 417 and 418. *Subduction Top to Bottom*, 19–38. https://doi.org/10.1029/GM096p0019
Stevens, T. O., & McKinley, J. P. (2000). Abiotic controls on H_2 production from Basalt− Water reactions and implications for aquifer biogeochemistry. *Environmental Science & Technology*, *34*(5), 826–831. https://doi.org/10.1021/es990583g
Stolper, D. A., & Bucholz, C. E. (2019). Neoproterozoic to early Phanerozoic rise in island arc redox state due to deep ocean oxygenation and increased marine sulfate levels. *Proceedings of the National Academy of Sciences*, *116*(18), 8746–8755. https://doi.org/10.1073/pnas.1821847116
Stolper, D. A., Higgins, J. A., & Derry, L. A. (2021). The role of the solid Earth in regulating atmospheric O_2 levels. *American Journal of Science*, *321*(10), 1381–1444. https://doi.org/10.2475/10.2021.01
Stolper, D. A., & Keller, C. B. (2018). A record of deep-ocean dissolved O_2 from the oxidation state of iron in submarine basalts. *Nature*, *553*(7688), 323–327. https://doi.org/10.1038/nature25009
Swanson-Hysell, N. L., & Macdonald, F. A. (2017). Tropical weathering of the Taconic orogeny as a driver for Ordovician cooling. *Geology*, *45*(8), 719–722. https://doi.org/10.1130/G38985.1
Taylor, B., & Martinez, F. (2003). Back-arc basin basalt systematics. *Earth and Planetary Science Letters*, *210*(3–4), 481–497. https://doi.org/10.1016/S0012-821X(03)00167-5
Tostevin, R., & Mills, B. J. (2020). Reconciling proxy records and models of Earth's oxygenation during the Neoproterozoic and Palaeozoic. *Interface Focus*, *10*(4), 20190137. https://doi.org/10.1098/rsfs.2019.0137
Varne, R., Brown, A. V., & Falloon, T. (2000). *Macquarie island: Its geology, structural history, and the timing and tectonic setting of its N-MORB to E-MORB magmatism*. Special Papers-Geological Society of America. 301–320.
Wallace, M. W., Shuster, A., Greig, A., Planavsky, N. J., & Reed, C. P. (2017). Oxygenation history of the Neoproterozoic to early Phanerozoic and the rise of land plants. *Earth and Planetary Science Letters*, *466*, 12–19. https://doi.org/10.1016/j.epsl.2017.02.046
Williams, H. (1973). Bay of islands map-area, Newfoundland: Canada geology. *Survey Paper*, *72*(34), 7.
Williams, H., & Malpas, J. (1972). Sheeted dikes and brecciated dike rocks within transported igneous complexes Bay of Islands, Western Newfoundland. *Canadian Journal of Earth Sciences*, *9*(9), 1216–1229. https://doi.org/10.1139/e72-105
Wilson, A. D. (1960). The micro-determination of ferrous iron in silicate minerals by a volumetric and a colorimetric method. *Analyst*, *85*(1016), 823–827. https://doi.org/10.1039/AN9608500823
Wood, R., Donoghue, P. C., Lenton, T. M., Liu, A. G., & Poulton, S. W. (2020). The origin and rise of complex life: Progress requires interdisciplinary integration and hypothesis testing. *Interface Focus*, *10*(4), 20200024. https://doi.org/10.1098/rsfs.2020.0024
Yan, W., & Casey, J. F. (2020). A new concordia age for the 'forearc' Bay of Islands Ophiolite Complex, Western Newfoundland utilizing spatially-resolved LA-ICP-MS U-Pb analyses of zircon. *Gondwana Research*, *86*, 1–22. https://doi.org/10.1016/j.gr.2020.05.007
Yeung, L. Y. (2017). Low oxygen and argon in the Neoproterozoic atmosphere at 815 Ma. *Earth and Planetary Science Letters*, *480*, 66–74. https://doi.org/10.1016/j.epsl.2017.09.044
Zhang, H. L., Cottrell, E., Solheid, P. A., Kelley, K. A., & Hirschmann, M. M. (2018). Determination of $Fe^{3+}/\Sigma Fe$ of XANES basaltic glass standards by Mössbauer spectroscopy and its application to the oxidation state of iron in MORB. *Chemical Geology*, *479*, 166–175. https://doi.org/10.1016/j.chemgeo.2018.01.006